Table 2. No. of patients with drug-related adverse events that occurred in ≥20% of patients receiving lapatinib

	Dose (mg/day)[a]												No. of patients (%)
	900			1200			1600			1800			
Common terminology criteria grade	1	2	3	1	2	3	1	2	3	1	2	3	
Any adverse events	3	3	0	4	2	0	1	4	1	2	2	2	24 (100)
Gastrointestinal	1	1	0	4	0	0	2	3	1	3	1	2	18 (75)
Diarrhea	1	1	0	4	0	0	2	1	1	3	1	2	16 (67)
Stomatitis	0	0	0	1	0	0	1	2	0	1	0	0	5 (21)
Skin	4	2	0	3	1	0	4	2	0	4	2	0	22 (92)
Rash	1	0	0	4	0	0	1	2	0	3	2	0	13 (54)
Dry skin	5	0	0	2	0	0	1	0	0	0	0	0	8 (33)
Seborrheic dermatitis	3	1	0	0	0	0	0	0	0	1	0	0	5 (21)
Paronychia	0	1	0	0	1	0	2	0	0	1	0	0	5 (21)
Metabolism and nutrition	1	0	0	1	0	0	2	0	0	4	0	0	8 (33)
Anorexia	0	0	0	1	0	0	1	0	0	3	0	0	5 (21)
Investigations	2	1	0	3	2	0	3	1	0	3	1	1	17 (71)
Decreased lymphocyte count	0	1	0	1	1	0	0	1	0	1	0	0	5 (21)

[a]Six patients at each dose level.

patients at each dose level. The majority of events was mild (Grade 1–2); the most common events were skin reactions (mostly rash and dry skin) observed in 22 patients (92%) and gastrointestinal disorders (mostly diarrhea) in 18 patients (75%). The most severe drug-related adverse events were Grade 3 diarrhea observed in one patient at 1600 mg dose level and two patients at 1800 mg dose level. One of these also had Grade 3 γ-GTP increase. All diarrhea resolved with routine symptomatic treatment during or after withdrawal of lapatinib therapy, γ-GTP increase resolved without further treatment after completion of lapatinib therapy.

Grade 1/2 drug-related nausea and vomiting were experienced only by patients at higher dose levels of lapatinib [1/6 (17%) at 1600 mg/day and 3/6 (50%) at 1800 mg/day], with Grade 2 symptoms only seen at the 1800 mg dose level.

For other adverse events, no clear drug relation was found. The most frequent events included decreased body weight and serum alkaline phosphatase increase, each observed in 10 patients (42%). Grade 1 drug-related decreases in left ventricular ejection fraction were found in three of the six patients at the 1200 mg dose level. No clinically relevant changes in vital signs, 12-lead electrocardiogram or echocardiography were noted.

Hypoxemia and pneumonia were reported at the 900-mg dose level in another patient with NSCLC on Day 35. After hypoxemia occurred, the patient continued to receive study drug medication until Day 40. We attributed hypoxemia to bronchostenosis caused by the primary disease. Oxygen inhalation and erythromycin were given and hypoxemia improved while the pneumonia was resolved on Day 41 before the patient died from progression of primary disease 3 months after the events were resolved. Chest X-rays and CT findings for this patient were inconsistent with those for interstitial pneumonia associated with other tyrosine kinase inhibitors; therefore a drug relation with lapatinib was denied.

Maximum Tolerated Dose

Dose escalation was stopped at 1800 mg/day, where two patients experienced DLT (Grade 3 diarrhea). One of these patients also experienced Grade 3 γ-GTP increase. Thus, 1800 mg/day was determined as the MTD.

Pharmacokinetics

Table 3 shows the PK parameters derived from data on 23 patients (data from one patient received lapatinib for only 19 days and are not included).

Serum concentrations of lapatinib at each dose level on Days 1 and 21 are shown in Fig. 1. Repeated doses of lapatinib (900–1800 mg/day) for 21 days resulted in dose-related increases in mean C_{max} (range, 1715–3111 ng/ml) and mean AUC_{0-24} (range, 25 680–51 099 ng·h/ml) (Table 3). Large inter-patient variations were found in mean C_{max} and mean AUC_{0-24}. After a single dose of lapatinib, t_{max} was ~4 h, although values varied greatly among patients. After 21 days of treatment, t_{max} values were similar to those observed after the single dosing on Day 1.

Table 3. Derived pharmacokinetic parameters of lapatinib (including 95% confidence intervals)

Dose (mg/day)[a]	Geometric mean C_{max} (ng/ml)		Mean CSS_{max} (ng/ml)	Median t_{max} (h)		Geometric mean AUC (h ng/ml)[b]		Median $t_{1/2}$ (h)	
	Day 1	Day 21	Day 21	Day 1	Day 21	Day 1	Day 21	Day 1	Day 21
900	1011 (694–1472)	1895 (1319–2721)	857 (386–1234)	4.0 (2.0–6.0)	4.0 (3.0–6.0)	17 577 (11 812–26 154)	29 272 (21 618–39 638)	12.9 (10.1–18.3)	23.1 (9.8–38.2)
1200	1027 (474–2227)	1715 (965–3048)	820 (226–1308)	3.5 (2.1–6.0)	3.6 (3.0–7.9)	15 441 (7410–32 176)	25 680 (13 728–48 038)	11.5 (10.1–19.5)	16.9 (15.1–34.3)
1600	1538 (1042–2268)	3111 (1937–4996)	1899 (818–4357)	4.0 (2.0–8.0)	5.1 (0.9–8.0)	26 361 (17 519–39 665)	51 099 (28 674–91 062)	13.9 (9.6–18.0)	26.2 (12.9–48.3)
1800	1227 (465–3242)	2333 (927–5870)	1528 (586–3393)	3.9 (3.0–8.0)	3.9 (3.0–7.3)	32 841 (18 884–57 114)	39 451 (14 909–104 391)	15.7 (11.0–133.1)	21.8 (18.5–104.5)

AUC, area under the plasma drug concentration–time curve; C_{max}, maximum serum concentration; CSS_{max}, mean steady state maximum serum concentration; t_{max}, time to reach C_{max}; $t_{1/2}$, terminal half-life.
[a]Six patients at 900, 1200 and 1600 mg/day and five at 1800 mg/day.
[b]Day 1, AUC from 0 to infinity; Day 21, AUC from 0 to 24 h.

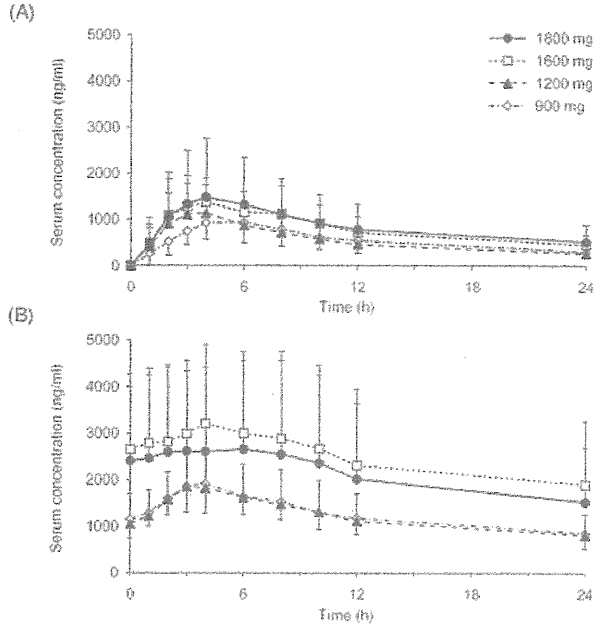

Figure 1. Serum concentrations of lapatinib at each dose level as detected on (A) Day 1 and (B) Day 21.

Steady-state serum concentrations of lapatinib generally increased with dose, 820 ± 448 ng/ml at 1200 mg dose level and 1899 ± 1356 ng/ml at 1600 mg dose level (Table 3). Both concentrations exceeded the half maximal inhibitory concentration values for *in vitro* tumor growth (14). The median $t_{1/2}$ after repeat dose was 16.9 h (range, 15.1–34.3) at 1200 mg dose level and 26.2 h (range, 12.9–48.3) at 1600 mg dose level.

The fraction of urinary excretion of lapatinib was <0.1% of the dose, suggesting that none or negligible amount of drug is excreted in urine.

Comparison of on-treatment C_{max} and AUC_{0-24} values obtained in Japanese and western patients are shown in Fig. 2 (43,44).

Efficacy

Among 24 patients, the best overall response was assessed as partial response (PR) in two patients (8.3%), stable disease (SD) in 12 patients (50.0%), progressive disease in eight patients (33.3%) and indeterminate in two patients (8.3%).

Of the two patients with PR, the first was a 73-year-old man with NSCLC (squamous cell carcinoma) with prior docetaxel and gemcitabine treatment, who received lapatinib 900 mg/day. PR was assessed by CT scan with 41% shrinkage on Day 49. Time to progression was 191 days. The second patient was a 55-year-old woman with trastuzumab-resistant breast cancer (invasive ductal carcinoma; hormone receptor-negative, ErbB-2 3+). Disease progressed after doxorubicin and cyclophosphamide/docetaxel therapy, was

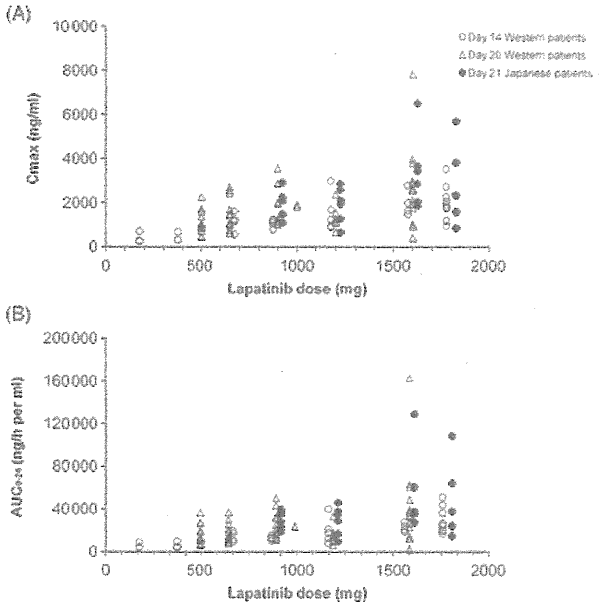

Figure 2. Relation between dose of lapatinib and exposure: comparison of (A) maximum serum concentration (C_{max}) and (B) area under the plasma drug concentration–time curve from 0 to 24 h (AUC_{0-24}) after dosing on Day 21 (our study, Japanese patients) and Days 14 and 20 (US studies, western patients).

stable with doxifluridine, and progressed with trastuzumab. Following treatment with lapatinib 1600 mg/day, the tumor shrank by 41% on Day 21. Time to progression was 133 days.

Among the patients with SD, three (two with NSCLC and one with colorectal cancer) were stabilized for >6 months and three (two with NSCLC and one with cervical cancer) were stabilized for 3–6 months and therefore were considered as having a durable response.

DISCUSSION

The dual ErbB-1/-2 inhibitor lapatinib taken orally once daily for ≥21 days was well tolerated at doses of 900–1600 mg in Japanese solid tumor patients. Adverse events were mostly mild in nature, and only four grade ≥3 drug-related adverse events were noted, in three patients (three events of Grade 3 diarrhea and one Grade 3 γ-GTP increase). No NCI-CTC Grade 4 adverse events were observed. Grade 1–2 diarrhea occurred in some patients other than those who experienced Grade 3 diarrhea; for these, supportive therapy was given and fully recovered in all cases. Grade 1/2 drug-related nausea and vomiting were experienced only by patients at higher dose levels of lapatinib, with Grade 2 symptoms only seen at 1800 mg dose level.

The types and incidences of drug-related adverse events in Japanese patients were similar to those reported from studies conducted in healthy volunteers (18) and two overseas Phase I studies, the latter including a parallel study in western patients that used similar dose administration and dose-escalation schedules (43,44). In that study as well as in ours, diarrhea and rash were the most frequently noted drug-related adverse events. Adverse events were generally mild (Grade 1–2), transient and reversible on dose delay or interruption. Headache, which was common in western patients (18), was reported only by one patient at 1600 mg dose level. 1800 mg/day was considered as MTD, at which Grade 3 diarrhea and γ-GTP increase were observed.

Skin-related adverse events of lapatinib were similar to those reported for other agents that target ErbB-1; rash is also a common adverse event associated with the ErbB-1 tyrosine kinase inhibitors gefitinib (46–49) and erlotinib (7,50), as well as the anti-ErbB-1 antibody cetuximab (51). Patients who received these medications also experienced diarrhea (7,46–50). These adverse events occurred at a similar frequency in our study as in two overseas Phase I studies (43,44).

Apart from one event of γ-GTP increase, no Grade ≥3 abnormal laboratory test suggestive of liver dysfunction was noted. Therefore, drug-related liver abnormality was generally less frequently seen with lapatinib compared with gefitinib (48,49).

Hematologic toxicity was uncommon and limited to cases of anemia. This finding is similar to those of the Phase I biomarker study (44) and studies of gefitinib (48,49,52).

None of the patients developed interstitial lung disease, which is an adverse event reportedly associated with gefitinib (53,54) and occurs in 5.8% of Japanese patients (55). However, because of the limited number of patients in our study, further studies are required to assess safety of lapatinib in this regard.

Cardiotoxicity is a known adverse event associated with trastuzumab therapy and might be related to ErbB-2 inhibition (2,56); however, we found no evidence of drug-related cardiac dysfunction in our study.

PK parameters such as C_{max} and AUC_{0-24} in this study were analyzed and their means and 95% confidence intervals compared with those obtained at similar doses (900–1800 mg) in two overseas Phase I studies (43,44). As can be seen in Fig. 2, the values were comparable among the three studies. However, large inter-patient variations were noted, especially in Japanese patients, and these might have contributed to higher mean values. On the other hand, no clear pharmacokinetic differences were apparent between Japanese and non-Japanese subjects, suggesting that values obtained overseas can be extrapolated to the Japanese population.

The dose recommended for further clinical studies outside Japan, 1500 mg/day, can be used for Phase II studies in Japan. We base this recommendation on the similar PK profiles of lapatinib in Japanese and western patients, evidence of antitumor activity at doses of ≥900 mg/day, and an MTD of 1800 mg/day.

To conclude, lapatinib, taken continuously as once-daily oral therapy at 900–1600 mg, was well tolerated in Japanese

patients with solid tumors. The safety and PK profiles shown in this study are similar to those in Phase I studies conducted in western patients. Phase II studies to determine the efficacy of lapatinib against a range of tumors are now in progress.

Acknowledgements

We thank all the patients who participated in this study, their families, and all the investigators (Dr K. Araki, Dr M. Fukuda, Dr M. Ikeda, Dr H. Kaneda, Dr T. Sato, Dr M. Tahara and Dr K. Tamura), research nurses, and study coordinators at study sites.

Funding

This study was sponsored by GlaxoSmithKline K.K.

Conflict of interest statement

The author, Hironobu Minami, receives honoraria from GlaxoSmithKline. The authors, Masayuki Kanezaki, Akihira Mukaiyama, and Yoshiyuki Minamide are employed by GlaxoSmithKline.

References

1. Yarden Y, Sliwkowski MX. Untangling the ErbB signalling network. *Nat Rev Mol Cell Biol* 2001;2:127–37.
2. Horton J. Trastuzumab use in breast cancer: clinical issues. *Cancer Control* 2002;9:499–507.
3. Sridhar SS, Seymour L, Shepherd FA. Inhibitors of epidermal-growth-factor receptors: a review of clinical research with a focus on non-small-cell lung cancer. *Lancet Oncol* 2003;4:397–406.
4. Rocha-Lima CM, Soares HP, Raez LE, Singal R. EGFR targeting of solid tumors. *Cancer Control* 2007;14:295–304.
5. Baselga J, Averbuch SD. ZD1839 ('Iressa') as an anticancer agent. *Drugs* 2000;60(Suppl. 1):33–40. Discussion 41–2.
6. Baselga J, Pfister D, Cooper MR, Cohen R, Burtness B, Bos M, et al. Phase I studies of anti-epidermal growth factor receptor chimeric antibody C225 alone and in combination with cisplatin. *J Clin Oncol* 2000;18:904–14.
7. Hidalgo M, Siu LL, Nemunaitis J, Rizzo J, Hammond LA, Takimoto C, et al. Phase I and pharmacokinetic study of OSI-774, an epidermal growth factor receptor tyrosine kinase inhibitor, in patients with advanced solid malignancies. *J Clin Oncol* 2001;19:3267–79.
8. Fry DW. Mechanism of action of erbB tyrosine kinase inhibitors. *Exp Cell Res* 2003;284:131–9.
9. Veronese ML, O'Dwyer PJ. Monoclonal antibodies in the treatment of colorectal cancer. *Eur J Cancer* 2004;40:1292–301.
10. Esteva FJ. Monoclonal antibodies, small molecules, and vaccines in the treatment of breast cancer. *Oncologist* 2004;9(Suppl. 3):4–9.
11. Simpson BJ, Phillips HA, Lessells AM, Langdon SP, Miller WR. c-erbB growth-factor-receptor proteins in ovarian tumors. *Int J Cancer* 1995;64:202–6.
12. Cohen BD, Kiener PA, Green JM, Foy L, Fell HP, Zhang K. The relationship between human epidermal growth–like factor receptor expression and cellular transformation in NIH3T3 cells. *J Biol Chem* 1996;271:30897–903.
13. Suo Z, Risberg B, Kalsson MG, Willman K, Tierens A, Skovlund E, et al. EGFR family expression in breast carcinomas. c-erbB-2 and c-erbB-4 receptors have different events on survival. *J Pathol* 2002;196:17–25.
14. Rusnak DW, Lackey K, Affleck K, Wood ER, Alligood KJ, Rhodes N, et al. The effects of the novel, reversible epidermal growth factor receptor/ErbB-2 tyrosine kinase inhibitor, GW2016, on the growth of human normal and tumor-derived cell lines *in vitro* and *in vivo*. *Mol Cancer Ther* 2001;1:85–94.
15. Xia W, Mullin RJ, Keith BR, Liu L-H, Ma H, Rusnak DW, et al. Anti-tumor activity of GW572016: a dual tyrosine kinase inhibitor blocks EGF activation of EGFR/erbB2 and downstream Erk1/2 and AKT pathways. *Oncogene* 2002;21:6255–63.
16. Wood ER, Truesdale AT, McDonald OB, Yuan D, Hassell A, Dickerson SH, et al. A unique structure for epidermal growth factor receptor bound to GW572016 (lapatinib): relationships among protein conformation, inhibitor off-rate, and receptor activity in tumor cells. *Cancer Res* 2004;64:6652–9.
17. Xia W, Liu L-H, Ho P, Spector NL. Truncated ErbB2 receptor ($p95^{ErbB2}$) is regulated by heregulin through heterodimer formation with ErbB3 yet remains sensitive to the dual EGFR/ErbB2 kinase inhibitor GW572016. *Oncogene* 2004;23:646–53.
18. Bence AK, Anderson EB, Halepota MA, Doukas MA, DeSimone PA, Davis GA, et al. Phase I pharmacokinetic studies evaluating single and multiple doses of oral GW572016, a dual EGFR–ErbB2 inhibitor, in healthy subjects. *Invest New Drugs* 2005;23:39–49.
19. Raymond E, Faivre S, Armand JP. Epidermal growth factor receptor tyrosine kinase as a target for anticancer therapy. *Drugs* 2000;60(Suppl. 1):15–23.
20. Duda RB, Cundiff D, August CZ, Wagman LD, Bauer KD. Growth factor receptor and related oncogene determination in mesenchymal tumors. *Cancer* 1993;71:3526–30.
21. Rieske P, Kordek R, Bartkowiak J, Debiec-Rychter M, Biernat W, Liberski PP. A comparative study of epidermal growth factor receptor (EGFR) and MDM2 gene amplification and protein immunoreactivity in human glioblastomas. *Pol J Pathol* 1998;49: 145–9.
22. Hoffmann TK, Balló H, Braunstein S, Van Lierop A, Wagenmann M, Bier H. Serum level and tissue expression of c-erbB-1 and c-erbB-2 proto-oncogene products in patients with squamous cell carcinoma of the head and neck. *Oral Oncol* 2001;37:50–6.
23. Wang W, Johansson HE, Bergholm UI, Westermark KM, Grimelius LE. Expression of c-Myc, TGF-alpha and EGF-receptor in sporadic medullary thyroid carcinoma. *Acta Oncol* 1997;36:407–11.
24. Iihara K, Shiozaki H, Tahara H, Kobayashi K, Inoue M, Tamura S, et al. Prognostic significance of transforming growth factor-alpha in human esophageal carcinoma. Implication for the autocrine proliferation. *Cancer* 1993;71:2902–9.
25. Lee CS, Pirdas A. Epidermal growth factor receptor immunoreactivity in gallbladder and extrahepatic biliary tract tumours. *Pathol Res Pract* 1995;191:1087–91.
26. Yoshida K, Hosoya Y, Sumi S, Honda M, Moriguchi H, Yano M, et al. Studies of the expression of epidermal growth factor receptor in human renal cell carcinoma: a comparison of immunohistochemical method versus ligand binding assay. *Oncology* 1997;54:220–5.
27. Sriplakich S, Jahnson S, Karlsson MG. Epidermal growth factor receptor expression: predictive value for the outcome after cystectomy for bladder cancer? *BJU Int* 1999;83:498–503.
28. Kim JW, Kim YT, Kim DK. Correlation between EGFR and c-erbB-2 oncoprotein status and response to neoadjuvant chemotherapy in cervical carcinoma. *Yonsei Med J* 1999;40:207–14.
29. Miturski R, Semczuk A, Postawski K, Jakowicki JA. Epidermal growth factor receptor immunostaining and epidermal growth factor receptor-tyrosine kinase activity in proliferative and neoplastic human endometrium. *Tumour Biol* 2000;21:358–66.
30. Scholes AG, Hagan S, Hiscott P, Damato BE, Grierson I. Overexpression of epidermal growth factor receptor restricted to macrophages in uveal melanoma. *Arch Ophthalmol* 2001;119:373–7.
31. Beech D, Pollock RE, Tsan R, Radinsky R. Epidermal growth factor receptor and insulin-like growth factor-I receptor expression and function in human soft-tissue sarcoma cells. *Int J Oncol* 1998;12: 329–36.
32. Oda Y, Wehrmann B, Radig K, Walter H, Röse I, Neumann W, et al. Expression of growth factors and their receptors in human osteosarcomas. Immunohistochemical detection of epidermal growth factor, platelet-derived growth factor and their receptors: its correlation with proliferating activities and p53 expression. *Gen Diagn Pathol* 1995;141:97–103.

33. Koeppen HK, Wright BD, Burt AD, Quirke P, McNicol AM, Dybdal NO, et al. Overexpression of HER2/neu in solid tumours: an immunohistochemical survey. *Histopathology* 2001;38: 96–104.
34. Press MF, Pike MC, Hung G, Zhou JY, Ma Y, George J, et al. Amplification and overexpression of HER-2/neu in carcinomas of the salivary gland: correlation with poor prognosis. *Cancer Res* 1994;54:5675–82.
35. Haugen DR, Akslen LA, Varhaug JE, Lillehaug JR. Expression of c-erbB-2 protein in papillary thyroid carcinomas. *Br J Cancer* 1992;65:832–7.
36. Lam KY, Tin L, Ma L. C-erbB-2 protein expression in oesophageal squamous epithelium from oesophageal squamous cell carcinomas, with special reference to histological grade of carcinoma and pre-invasive lesions. *Eur J Surg Oncol* 1998;24:431–5.
37. Herrera GA. C-erb B-2 amplification in cystic renal disease. *Kidney Int* 1991;40:509–13.
38. Rolitsky CD, Theil KS, McGaughy VR, Copeland LJ, Niemann TH. HER-2/neu amplification and overexpression in endometrial carcinoma. *Int J Gynecol Pathol* 1999;18:138–43.
39. Leng J, Lang J, Shen K, Guo L. Overexpression of p53, EGFR, c-erbB2 and c-erbB3 in endometrioid carcinoma of the ovary. *Chin Med Sci J* 1997;12:67–70.
40. Foster H, Ganti AK, Knox S, Hebert B, Tendulkar K, Fraiman GN, et al. Determination and role of HER-2/neu overexpression in soft tissue sarcomas. *Proc Am Soc Clin Oncol* 2002;21: (Abstract 1622).
41. World Medical Association. World Medical Association Declaration of Helsinki. 2004. Available at: http://www.wma.net/e/policy/b3.htm.
42. Japan Ministry of Health and Welfare. Good clinical practice for trials on drugs. Ordinance no. 28. Tokyo, Japan Ministry of Health and Welfare 1997.
43. Versola M, Burris HA, Jones S, Wilding G, Taylor C, Pandite L, et al. Clinical activity of GW572016 in EGF10003 in patients with solid tumors. *Proc Am Soc Clin Oncol* 2004;23: (Abstract 3047).
44. Burris HA, III, Hurwitz HI, Dees EC, Dowlati A, Blackwell KL, O'Neil B, et al. Phase I safety, pharmacokinetics, and clinical activity study of lapatinib (GW572016), a reversible dual inhibitor of epidermal growth factor receptor tyrosine kinases, in heavily pretreated patients with metastatic carcinomas. *J Clin Oncol* 2005;23:5305–13.
45. Therasse P, Arbuck SG, Eisenhauer EA, Wanders J, Kaplan RS, Rubinstein L, et al. New guidelines to evaluate the response to treatment in solid tumors. European Organization for Research and Treatment of Cancer, National Cancer Institute of the United States, National Cancer Institute of Canada. *J Natl Cancer Inst* 2000;92:205–16.
46. Baselga J, Rischin D, Ranson M, Calvert H, Raymond E, Kieback DG, et al. Phase I safety, pharmacokinetic, and pharmacodynamic trial of ZD1839, a selective oral epidermal growth factor receptor tyrosine kinase inhibitor, in patients with five selected tumor types. *J Clin Oncol* 2002;20:4292–302.
47. Herbst RS, Maddox A-M, Rothenberg ML, Small EJ, Rubin EH, Baselga J, et al. Selective oral epidermal growth factor receptor tyrosine kinase inhibitor ZD1839 is generally well-tolerated and has activity in non-small-cell lung cancer and other solid tumors: results of a phase I trial. *J Clin Oncol* 2002;20:3815–25.
48. Fukuoka M, Yano S, Giaccone G, Tamura T, Nakagawa K, Douillard J-Y, et al. Multi-institutional randomized phase II trial of gefitinib for previously treated patients with advanced non-small-cell lung cancer (the IDEAL 1 trial). *J Clin Oncol* 2003;21:2237–46.
49. Nakagawa K, Tamura T, Negoro S, Kudoh S, Yamamoto N, Yamamoto N, et al. Phase I pharmacokinetic trial of the selective oral epidermal growth factor receptor tyrosine kinase inhibitor gefitinib ('Iressa', ZD1839) in Japanese patients with solid malignant tumors. *Ann Oncol* 2003;14:922–30.
50. Yamamoto N, Horiike A, Fujisaka Y, Murakami H, Shimoyama T, Yamada Y, et al. Phase I dose-finding and pharmacokinetic study of the oral epidermal growth factor receptor tyrosine kinase inhibitor Ro50-8231 (erlotinib) in Japanese patients with solid tumors. *Cancer Chemother Pharmacol* 2008;61:489–96.
51. Busam KJ, Capodieci P, Motzer R, Kiehn T, Phelan D, Halpern AC. Cutaneous side-events in cancer patients treated with the antiepidermal growth factor receptor antibody C225. *Br J Dermatol* 2001;144: 1169–76.
52. Ranson M, Hammond LA, Ferry D, Kris M, Tullo A, Murray PI, et al. ZD1839, a selective oral epidermal growth factor receptor-tyrosine kinase inhibitor, is well tolerated and active in patients with solid malignant tumors: results of a phase I trial. *J Clin Oncol* 2002;20:2240–50.
53. Inoue A, Saijo Y, Maemondo M, Gomi K, Tokue Y, Kimura Y, et al. Severe acute interstitial pneumonia and gefitinib. *Lancet* 2003;361:137–9.
54. Takano T, Ohe Y, Kusumoto M, Tateishi U, Yamamoto S, Nokihara H, et al. Risk factors for interstitial lung disease and predictive factors for tumor response in patients with advanced non-small cell lung cancer treated with gefitinib. *Lung Cancer* 2004;45:93–104.
55. Yoshida S. The results of gefitinib prospective investigation. *Med Drug J* 2005;41:772–89.
56. Suter TM, Cook-Burns N, Barton C. Cardiotoxicity associated with trastuzumab (Herceptin) therapy in the treatment of metastatic breast cancer. *Breast* 2004;13:173–83.

Phase I Study of YM155, a Novel Survivin Suppressant, in Patients with Advanced Solid Tumors

Taroh Satoh,[1] Isamu Okamoto,[1] Masaki Miyazaki,[1] Ryotaroh Morinaga,[1] Asuka Tsuya,[1] Yoshikazu Hasegawa,[1] Masaaki Terashima,[1] Shinya Ueda,[1] Masahiro Fukuoka,[1] Yutaka Ariyoshi,[3] Toshikazu Saito,[4] Noriyuki Masuda,[5] Hirokazu Watanabe,[6] Tetsuo Taguchi,[2] Toru Kakihara,[7] Yumiko Aoyama,[7] Yohko Hashimoto,[7] and Kazuhiko Nakagawa[1]

Abstract

Purpose: YM155, a novel molecular targeted agent, suppresses survivin, a member of the inhibitor of apoptosis protein family that is overexpressed in many tumor types. The aim of this study was to determine the maximum tolerated dose (MTD) and to assess the safety, pharmacokinetics, and antitumor activity of YM155 in patients with advanced refractory solid tumors.

Experimental Design: Patients with advanced refractory solid tumors were treated with escalating doses of YM155 administered by continuous i.v. infusion for 168 hours in 21-day cycles.

Results: Of the 34 patients enrolled, 33 (median age, 59 years) received at least 1 dose of YM155 (range, 1-19 cycles). The dose levels studied were 1.8, 3.6, 4.8, 6.0, 8.0, and 10.6 mg/m^2/d. The MTD was determined to be 8.0 mg/m^2/d, based on a dose-limiting toxicity of increased blood creatinine observed in 2 patients receiving 10.6 mg/m^2/d. The most common adverse reactions judged to be related to YM155 were urine microalbumin present; fever; injection-site phlebitis; fatigue; and decreased hemoglobin/anemia, blood albumin, and lymphocyte count. The pharmacokinetic profile was almost linear over the dosing range and was similar between cycles 1 and 2. Urinary excretion of YM155 showed no definite difference among doses. Stable disease was achieved in nine patients.

Conclusions: YM155 was safely administered to patients with advanced refractory solid tumors by 168-hour continuous i.v. infusion in 21-day cycles. The MTD was determined to be 8.0 mg/m^2/d. The safety profile, plasma concentrations achieved, and antitumor activity observed merit further studies with this survivin suppressant, alone and in combination regimens.

Survivin, a member of the inhibitor of apoptosis family of proteins, is expressed during embryonic and fetal development, but is undetectable in normal adult human tissues, apart from thymus, placenta, CD34$^+$ cells, and some cells within the basal crypt layer of the gastrointestinal tract (1–5). *In vitro* studies suggest that survivin inhibits cell death induced via the extrinsic and intrinsic apoptotic pathways. In addition, survivin may also confer resistance to apoptosis by directly suppressing caspase activity (3). Overexpression of survivin has been shown in a variety of human cancers and is reportedly associated with a poor prognosis (6–13). It has been shown that the suppression of survivin induces tumor cell apoptosis and also enhances the sensitivity to apoptosis induced by existing anticancer drugs and other apoptotic stimuli (4, 14–16).

YM155 is a novel survivin suppressant that is currently in clinical development by Astellas Pharma, Inc. A preclinical study showed that YM155 suppressed both survivin protein and mRNA expression (17). In addition, sensitivity to YM155 was high in various human tumor cell lines such as hormone-refractory prostate cancer (17) and malignant lymphoma.[8] Furthermore, YM155 exerted greater antitumor activity compared with existing anticancer drugs, and YM155 concentrations were higher in tumor tissue than in plasma. In a toxicologic study, short-term exposure at high blood concentrations caused cardiotoxicity in the form of atrioventricular

Authors' Affiliations: [1]Department of Medical Oncology, Kinki University School of Medicine; and [2]Japan Society for Cancer Chemotherapy, Osaka, Japan; [3]Marumo Hospital, Aichi, Japan; [4]Social Insurance Chuo General Hospital; [5]Kitasato University School of Medicine; [6]National Cancer Center Hospital; and [7]Astellas Pharma, Inc., Tokyo, Japan

Received 7/14/08; revised 2/5/09; accepted 2/23/09; published OnlineFirst 5/26/09.
Grant support: Astellas Pharma, Inc.
The costs of publication of this article were defrayed in part by the payment of page charges. This article must therefore be hereby marked *advertisement* in accordance with 18 U.S.C. Section 1734 solely to indicate this fact.

Requests for reprints: Taroh Satoh, Department of Medical Oncology, Kinki University School of Medicine, Osaka, Japan. Phone: 81-72-366-0221; Fax: 81-72-360-5000; E-mail: taroh@med.kindai.ac.jp.

doi:10.1158/1078-0432.CCR-08-1946

[8] Unpublished data.

Translational Relevance

Survivin is a member of the inhibitor of apoptosis protein family that is overexpressed in many tumor types, and as such represents an excellent target for anticancer drug development. YM155 is a small molecule that suppresses survivin and has shown anticancer activity in a range of tumor cell lines *in vitro* and human tumor xenografts models *in vivo*. In this phase I study, YM155 was administered to 33 patients with advanced refractory solid tumors. YM155 seemed to be safe and well-tolerated, with a maximum tolerated dose of 8.0 mg/m^2/d. Stable disease was achieved in nine patients. The position of survivin as an anticancer drug target, together with the safety profile and antitumor activity in heavily pretreated patients with advanced refractory tumors shown in this phase I study, strongly supports the further evaluation of YM155, both as monotherapy and within combination regimens.

block and myocardial degeneration/necrosis, as well as nephrotoxicity, mainly displayed as proximal tubular necrosis and increased serum creatinine. In contrast, long-term exposure at low blood concentrations by 168-hour continuous infusion did not cause cardiotoxicity.[9]

Based on the differential expression of survivin in human malignancies and the negative prognostic role, together with preclinical antitumor activity and encouraging safety data, a phase I study of YM155 in patients with advanced solid tumors was conducted in Japan. The aim of this study was to determine the recommended dose and pharmacokinetic profile of YM155 and to evaluate its safety profile and antitumor effects.

Patients and Methods

Study design. This was an open-label, single-center, nonrandomized, phase I dose-escalation study. The primary objective was to assess the safety of YM155 administered to patients with advanced solid tumors. The secondary objectives included the investigation of the pharmacokinetic profile and tumor activity of YM155. After one cycle, patients could continue further treatment until either an unacceptable toxicity was experienced or disease progression occurred.

Inclusion and exclusion criteria. Eligibility criteria for patients enrolled in this study included refractory advanced solid tumors for which no standard therapy existed; histologic or cytologic diagnosis of cancer; at least 20 y of age; life expectancy of at least 12 wk; Eastern Cooperative Oncology Group performance status of <3; and adequate hematopoietic, hepatic, and renal functions (absolute neutrophil count of $\geq 1.5 \times 10^9$/L, platelets of $\geq 100 \times 10^9$/L, hemoglobin of ≥9 g/dL, bilirubin within 1.5× upper limit of normal, transaminases of ≤2.5× upper limit of normal, and creatinine of <1.5 × upper limit of normal). Patients must have discontinued all cancer therapies for at least 4 wk before study entry. Exclusion criteria included primary brain tumor or known central nervous system metastases, and uncontrolled clinically significant disease unrelated to the primary malignancy.

The study was approved by the ethics board of the participating center, and all patients gave written informed consent. The study was conducted in accordance with the Declaration of Helsinki and the applicable guidelines on good clinical practice.

Dosage and drug administration. YM155 was prepared for administration by dilution of an appropriate volume of concentrated stock solution in 5% dextrose in a light- and temperature-controlled environment. The diluted drug was administered via continuous i.v. infusion over 168 h, followed by 14-d observation (1 cycle). This method of administration was selected because toxicity studies using 168-h continuous infusion in dogs showed no cardiotoxicity and time-dependent antitumor activity.[10] A starting dose of 1.8 mg/m^2/d was chosen on the basis of toxicologic studies in rodents and the data from a U.S. phase I study (18). To avoid renal toxicity with YM155, patients were instructed to take sufficient quantities of water during administration of the drug.

Toxicity (tolerability and safety evaluation). The following safety assessments were done for each patient: subjective/objective symptoms, vital signs, laboratory tests, and 12-lead electrocardiogram. Adverse events were graded according to the Common Terminology Criteria for Adverse Events v3.0. Creatinine clearance was determined by the evaluation of fluctuations in urine creatinine and serum creatinine concentrations. A dose-limiting toxicity (DLT) was defined as an adverse drug reaction including nonhematologic toxicities ≥grade 3, except transient hyperglycemia and anorexia, and serum creatinine increased to ≥2.0 mg/dL; grade 4 hematologic toxicities, except a decreased neutrophil count of grade 4 (<500/μL) persisting for 5 d or less; nausea, vomiting, or diarrhea ≥grade 3 occurring despite prophylaxis after the first episode; and failure to satisfy the criteria for the next cycle within the specified period due to unresolved adverse drug reactions. The maximum tolerated dose (MTD) was defined as the dose that was one level lower than that at which DLT occurred in more than two of six patients.

Pharmacokinetics. The pharmacokinetic parameters of YM155 were evaluated during cycles 1 and 2. Venous blood samples, from a site other than the infusion site, were collected in tubes containing heparin sodium immediately before the start of the infusion (time 0): at 0.25, 0.5, 1, 2, 3, 4, 6, 12, 24, 48, 72, 96, 120, and 144 h after the start of infusion; at the end of infusion (168 h); and at the following times thereafter: 168.25, 168.5, 169, 170, 171, 172, 174, 180, 192, and 216 h. Samples were centrifuged immediately, and the resulting plasma was stored at −20°C before analysis. Urine samples were collected over 216 h after the start of continuous infusion to determine the urinary concentration of YM155 and were stored at −20°C before analysis.

Concentrations of YM155 were measured by Astellas Europe B.V. EDD using validated liquid chromatography tandem mass spectrometry procedures (18) and following Good Laboratory Practice.

The lower limits of quantitation for YM155 were 0.05 ng/mL in plasma and 1.0 ng/mL in urine. The concentrations are expressed as those of the cationic moiety of YM155.

Pharmacokinetic analysis was done in a model-independent manner using actual values of plasma concentration and actual time from the start of continuous infusion. Values below the lower limits of quantitation were treated as zero.

Efficacy (tumor assessment). Evaluations of lesions were done with computed tomography, magnetic resonance imaging, and bone scintigraphy, with tumor markers also evaluated. Assessment of antitumor activity was done in accordance with the Response Evaluation Criteria in Solid Tumors guidelines (19).

Results

Patients. A total of 34 patients were enrolled into 6 dosing cohorts between August 2004 and October 2006; 33 patients received at least 1 cycle of YM155. The demographic and baseline

[9] Unpublished data.

[10] Unpublished data.

Table 1. Patient demographics and disease characteristics

Characteristic	No. of patients
Total patients	33
Male/female	23/10
Age, y	
Median (range)	59 (26-81)
<65	25
≥65	8
ECOG performance status	
0	3
1	29
2	1
Tumor type	
NSCLC	7
Esophageal	6
Colorectal	4
Thymic	3
Thyroid	2
MFH	2
Pleural mesothelioma	2
Others*	7 (1 each)
Prior therapy	
Chemotherapy	32 (97.0%)
No. of prior regimens	
1	7
2	10
3	4
≥4	11
Radiation therapy	17 (51.5%)
Cancer-related surgery	19 (57.6%)

Abbreviations: ECOG, Eastern Cooperative Oncology Group; NSCLC, non–small cell lung cancer; MFH, malignant fibrous histiocytoma.
*Others: thymoma, synovial sarcoma, duodenal, double cancer of hypopharynx and thoracic esophageal cancer, paranasal sinus, pancreatic, and esophageal leiomyosarcoma.

patient characteristics are listed in Table 1. The most common malignancies in the 33 patients treated were non–small cell lung cancer (7 patients; 21.2%), esophageal cancer (6 patients; 18.2%), colorectal cancer (4 patients; 12.1%), and thymic cancer (3 patients; 9.1%). Thirty-two (97%) of the patients had at least 1 prior chemotherapy. Dose levels studied were 1.8, 3.6, 4.8, 6.0, 8.0, and 10.6 mg/m^2/d, and patients received 1 to 19 cycles of YM155.

DLT. The highest dose of YM155 administered was 10.6 mg/m^2/d, at which level 2 of 5 treated patients experienced a DLT of increased serum creatinine (accompanied by decreased lymphocyte count in 1 patient). Three of 5 patients in the 10.6 mg/m^2/d group had their dose reduced to 8.0 mg/m^2/d from cycle 2 onwards. At the 8.0 mg/m^2/d dose level, serum creatinine levels remained almost unchanged throughout the study. The MTD was therefore determined to be 8.0 mg/m^2/d. Additional DLTs were observed in one patient who received YM155 at the 6.0 mg/m^2/d dose level (grade 3 increased aspartate serum transferase) and in another patient whose dose was reduced to 8.0 mg/m^2/d (grade 4 anemia).

Safety. All 33 patients treated were included in the safety population. Throughout all treatment cycles, adverse events occurred in 97.0% (32 of 33 patients) and adverse drug reactions in 87.9% (29 of 33 patients) of all patients treated with YM155.

The most common drug-related adverse events (occurring in ≥15% of patients) were urine microalbumin present (12 patients; 36.4%), injection-site phlebitis (12 patients; 36.4%), fever (11 patients; 33.3%), decreased hemoglobin/anemia (9 patients; 27.3%), decreased lymphocyte count (8 patients; 24.2%), decreased blood albumin (8 patients; 24.2%), and fatigue (7 patients; 21.2%; Table 2). In most patients with decreased hemoglobin, reductions in hemoglobin were detected immediately after study drug initiation and were rated grade 1 or 2. The events recovered or remitted without treatment. Injection-site phlebitis was frequently reported in patients receiving infusion of lower doses of YM155 via peripheral veins. Consequently, infusion via a central vein was recommended for doses higher than 4.8 mg/m^2/d, which prevented the development of phlebitis.

The vast majority of drug-related adverse events (200 of 217, 92.2%) were judged to be grade 1 or 2 in severity. Grade 3 or 4 drug-related adverse events were reported in 8 patients. Grade 3 decreased lymphocyte count occurred in 6 patients, including 1

Table 2. Adverse events (≥15% incidence overall) related to YM155

Adverse event/YM155 dose (mg/m^2/d)	No. of patients experiencing toxicity during first course (all courses)													
	1.8 (*n* = 3)		3.6 (*n* = 6)		4.8 (*n* = 6)		6.0 (*n* = 7)		8.0 (*n* = 6)		10.6 (*n* = 5)		All (*n* = 33)	
Grade of adverse event	G1/2	G3	G1/2	G3	G1/2	G3	G1/2	G3	G1/2	G3	G1/2	G3/4	G1/2	G3/4
Urine microalbumin present	0	0	0(1)	0	1(1)	0	1(1)	0	4(4)	0	5(5)	0	11 (12)	0
Fever	0	0	1(2)	0	0	0	2(3)	0	2(2)	0	4(4)	0	9 (11)	0
Decreased hemoglobin/anemia	0	0	0(1)	0	1(1)	0	1(2)	0	1(1)	0	3(3)	1(1)*	6 (8)	1 (1)
Injection site phlebitis	2(3)	0	2(4)	0	2(2)	0	2(2)	0	0	0	0(1)†	0	8 (12)†	—
Fatigue	1(1)	0	0(1)	0	0(1)	0	1(1)	0	1(1)	0	2(2)	0	5 (7)	—
Decreased blood albumin	0	0	0	0	1(1)	0	1(1)	0	2(2)	0	4(4)	0	8 (8)	—
Decreased lymphocyte count	0	0	0	1(1)	0	1(1)	1(1)	0	0	1(1)	0	4(4)‡	1 (1)	7 (7)
Abnormal liver function test§	0(1)	0	0(1)	0	0	0	2(2)	1(1)	0	0	1(1)	0	3 (5)	1 (1)
Increased C-reactive protein	0	0	0	0	0	0	1	0	2	0	2(3)†	0	5 (6)†	—
Urine protein present	0	0	0	0	0	0	0	0	1	0	4	0	5 (5)	—

NOTE: * and ‡ are the same patient.
*Grade 4.
†An event after dose reduction to 8.0 mg/m^2/d in one patient.
‡Grade 4 in one patient.
§Abnormal liver function test includes increased aspartate, increased alanine serum transaminase, and increased γ-glutamyl transpeptidase.

each at YM155 doses of 3.6, 4.8, and 8.0 mg/m^2/d and 3 patients at the 10.6 mg/m^2/d YM155 dose level. A grade 4 decreased lymphocyte count was observed in an additional patient at the 10.6 mg/m^2/d dose level. Decreases in lymphocyte count were principally noted on day 3, and typically recovered without treatment during study drug administration, and without causing infection that might lead to study discontinuation. The remaining grade 3/4 drug-related adverse events included decreased hemoglobin/anemia [grade 4 in 1 patient in the 10.6 mg/m^2/d dose level (the same patient in which grade 4 lymphocyte count decreased was observed)] and abnormal liver function test (grade 3 in 1 patient in the 6.0 mg/m^2/d dose level).

The trial established kidney monitoring parameters for patients treated with YM155. Changes in renal parameters that occurred in 2 patients with a DLT in the 10.6 mg/m^2/d dose level in cycle 1 are shown in Fig. 1. Both patients had increased urine microalbumin at days 3 to 7, increased urinary protein at days 6 to 8, and increased serum creatinine and blood urea nitrogen at days 8 to 10 when administration

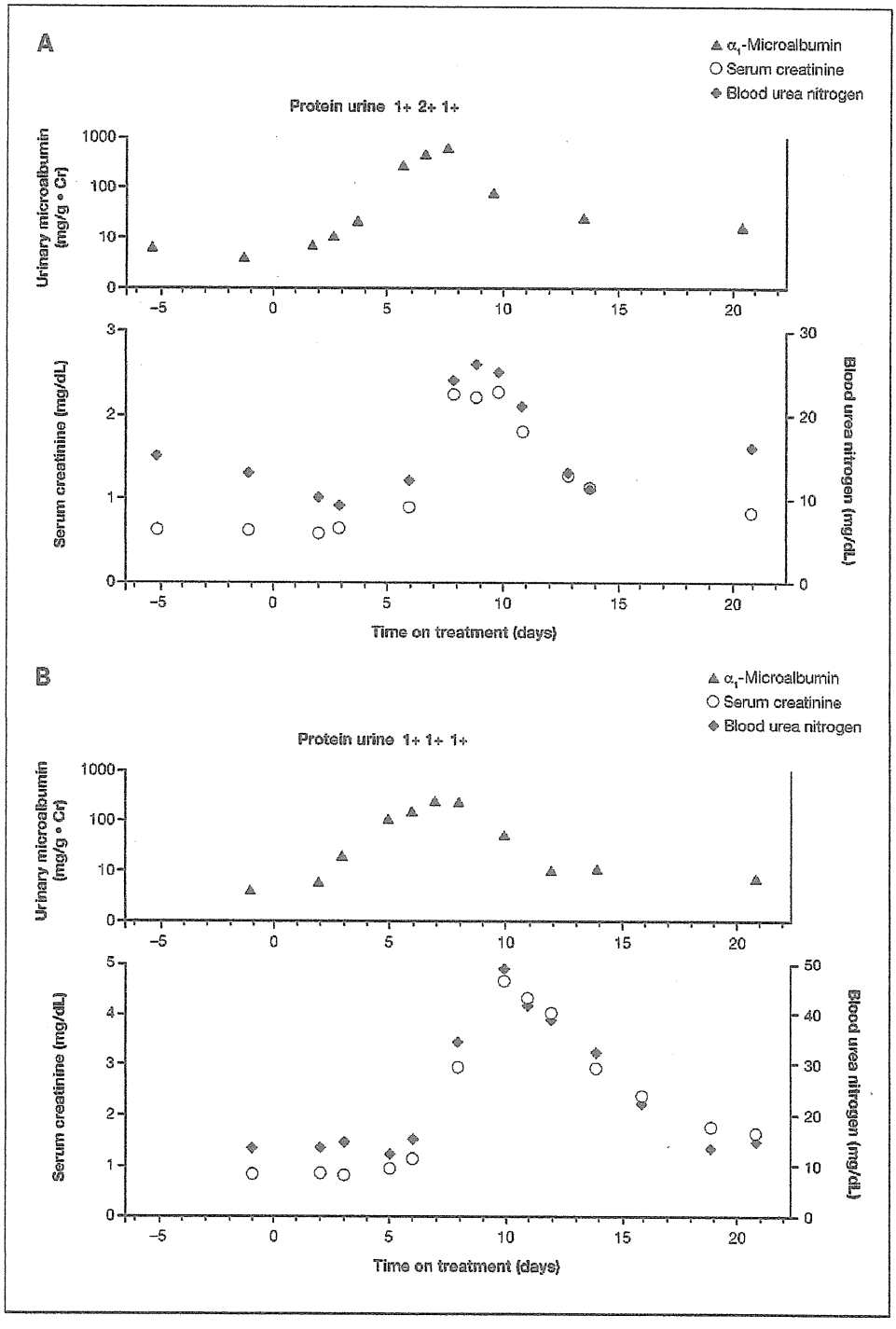

Fig. 1. Changes in renal parameters in patients in the 10.6 mg/m2/d group with thyroid cancer (*A*): esophageal canc -7, (*B*).

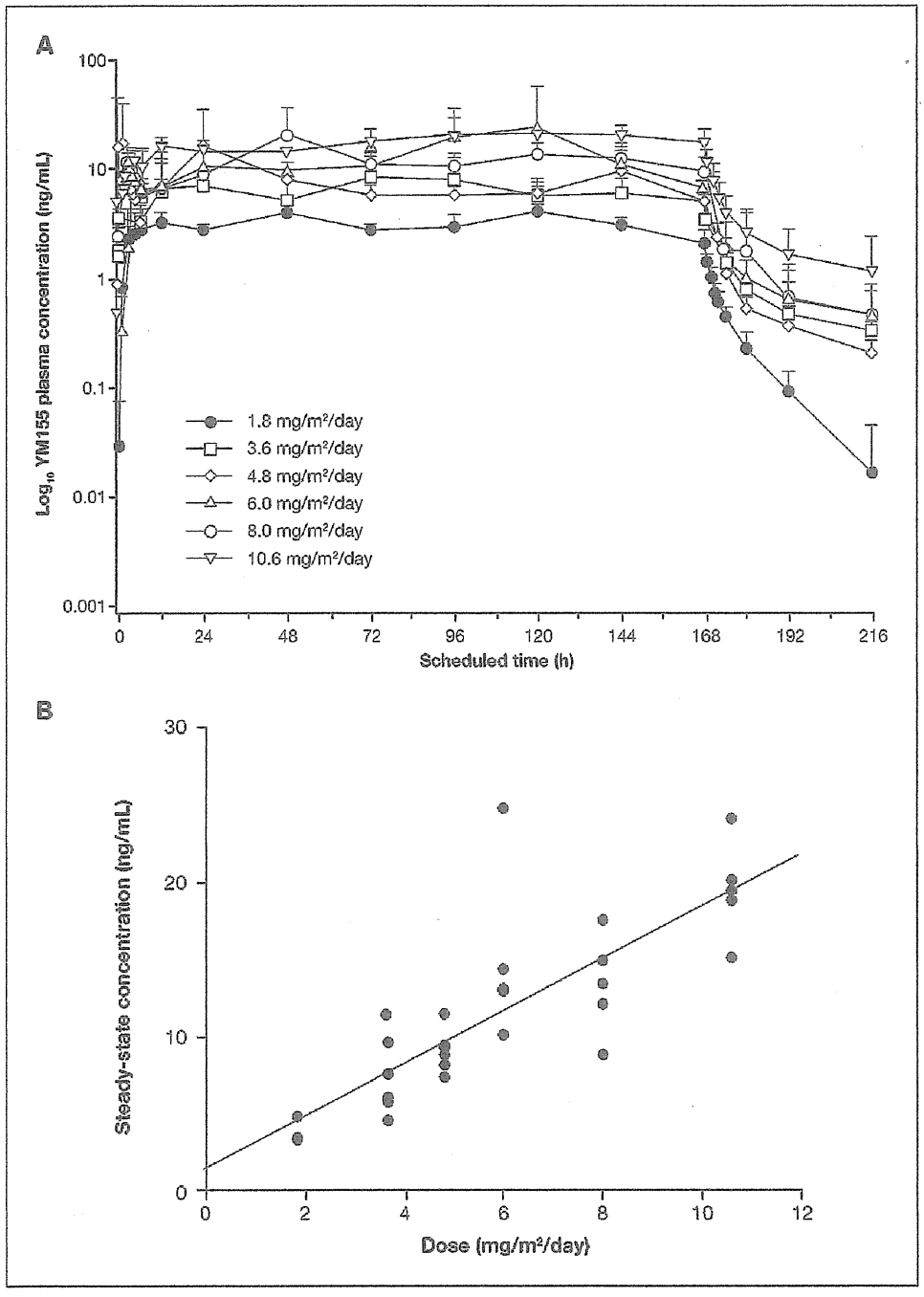

Fig. 2. YM155 plasma concentration. *A*, blood plasma concentrations of YM155 overtime. -h infusion were included; points, mean; bars, SD. *B*, dose versus change in steady-state blood plasma YM155 concentration. A total of 33 patients who completed 168-h infusion during cycle 1 were included.

had been completed. These changes were also temporally associated with decreased creatinine clearance and recovered after completion of administration. In contrast, changes in other parameters, including *N*-acetyl-D-glucosaminidase and α_1-microglobulin, were not consistently associated with renopathy and were not judged to be adverse events of clinical significance.

No other changes in safety variables, including vital signs, were considered to be clinically significant. Although atrial fibrillation on 12-lead electrocardiogram was judged to be an adverse drug reaction to YM155, this was only an asymptomatic finding of grade 1 severity and rapid recovery ensued. There were neither cumulative toxicities due to repeated cycles nor late-onset adverse events occurring in cycle 2 and beyond.

Fevers occurred mainly at days 2 to 4, with C-reactive protein increased. Part of them reached grade 2, but recovered during infusion of YM155 by nonsteroidal anti-inflammatory drugs.

Patient withdrawals. The majority of study discontinuations were due to disease progression (28 of 33 patients). In addition, 3 patients discontinued at their own request; one as a change of a therapy policy; and one as a result of an adverse event of aggravated superior vena caval syndrome, which was observed at a dose level of 4.8 mg/m^2/d, but causal relationship with the study drug was ruled out. Importantly, there were no treatment-related deaths.

Table 3. Tumors showing stable disease after therapy

YM155 dose (mg/m2/d)	Tumor type	No. of completed cycles
1.8	MFH	4
	Thymoma	6
3.6	NSCLC	3
	Synovial sarcoma	4
4.8	NSCLC	3
	Thymic	2
6.0	Thyroid	6
10.6	Esophageal leiomyosarcoma	3
	Thyroid	19

Pharmacokinetic analysis. Of the 33 patients who received at least 1 cycle of YM155, 31 provided full blood samples for pharmacokinetic analysis after a single cycle. The mean plasma concentration-time profiles of YM155 by dose after 168-hour infusion are shown in Fig. 2A. Plasma concentrations almost reached steady state about 24 hours after the start of infusion, with the area under the plasma concentration-time curve (from zero to the last quantifiable concentration) increasing with dose up to 10.6 mg/m^2/d. Mean plasma concentrations declined rapidly in a biphasic manner after the end of infusion. Mean values for an apparent elimination half-life ($t_{1/2}$) and total body clearance of YM155 seemed to be constant across the dose range. Steady-state concentration (C_{ss}) increased with dose up to 10.6 mg/m^2/d (Fig. 2B).

The fraction of dose excreted (F_e) in urine ranged from 25% to 42% and showed no relationship with the dose administered.

Although the dosing was based on body surface area, obvious correlation between body surface area and each pharmacokinetic parameter was unclear.[11]

Efficacy. External evaluation using computed tomography confirmed that 9 of 33 patients achieved stable disease with YM155 treatment (median duration, 81 days; range, 42-438 days; Table 3). The computed tomography images of two of the nine patients are shown in Fig. 3. One patient, a 47-year-old man with malignant fibrous histiocytoma (1.8 mg/m^2/d YM155 dose level), showed a 13% reduction in tumor size after cycle 1 (Fig. 3A and B). Another patient, a 56-year-old woman, had papillary cancer of the thyroid. This patient received 10.6 mg/m^2/d in cycle 1, which was reduced to 8.0 mg/m^2/d in cycle 2. Computed tomography after cycle 2 showed a 14% reduction in tumor size and disappearance of pleural effusion (Fig. 3C and D). External evaluation confirmed stable disease until 62 weeks.

The degree of unconfirmed response of all patients is displayed in the waterfall plot in Fig. 3E. Response was seen in a dose-independent manner.

Discussion

There has been much recent interest in the role of survivin as a potential molecular target in the treatment of cancer (20, 21). This is the result of the differential expression of survivin in human malignancies compared with normal adult tissues, the role of survivin in abrogating apoptosis signaling, and a growing body of promising preclinical data. Clearly, inhibition of survivin may induce tumor regression and, importantly, may increase the effectiveness of current therapies. As a result, YM155 is currently in clinical development as the first survivin suppressant.

In the present study, YM155 was administered by 168-hour continuous infusion to patients with refractory cancer or for whom there were no standard therapies available. The primary end point was an evaluation of the safety of this novel agent. The MTD of YM155 was determined to be 8.0 mg/m^2/d after the occurrence of a DLT of increased serum creatinine in 2 of 5 patients receiving 10.6 mg/m^2/d. In addition, most patients receiving this dose of YM155 showed a consistent tendency in the timing of renal abnormal changes. These results were consistent with the expected nephrotoxicity of YM155 following prior preclinical and clinical studies,[12] and further show the renal effects of YM155. None of the events in the present study led to severe renopathy, and renal parameters recovered in all cases. Increased urine microalbumin was observed at first, followed by increased urinary protein, and resulted in increased serum creatinine and blood urea nitrogen. This is indicative of early renal impairment because it occurs at the three highest doses. It was therefore considered that, by careful monitoring of renal parameters and taking appropriate measures in the event of abnormal changes, severe renopathy can be avoided. In addition, at the MTD of 8.0 mg/m^2/d, minimal changes in creatinine value were found. Increase of urine microalbumin and serum creatinine may suggest that the highest dose of YM155 influenced the glomerulus function. A nonrenal DLT of increased aspartate serum transferase was observed in 1 patient at the 6.0 mg/m^2/d dose level, which was below the MTD; however, this hepatopathy recovered after withdrawal of YM155. Results from a preclinical study have confirmed that the distribution of ^{14}C-YM155 is higher in the kidney and liver compared with other organs (15 and 5.2 times higher than in plasma, respectively), suggesting that this might be responsible for the observed renopathy and hepatopathy with YM155.[13]

In a preclinical study, cardiotoxicities were observed at a mean plasma YM155 C_{ss} of 188 ng/mL or higher. However, the mean C_{ss} in 7-day repeated infusion was 12.8 times the mean C_{ss} in 168-hour continuous infusion at the same total dose, which did not cause any cardiotoxicity.[14] In this study, even the highest dose of 10.6 mg/m^2/d produced only a mean C_{ss} of 19.20 ng/mL, and this did not result in any serious adverse event of cardiotoxicity.

The decreases in hemoglobin/anemia that were frequently observed at the higher doses of YM155 used in this study were typified by a decrease in hemoglobin immediately after the start of study drug administration in almost all patients, given that it is generally not until about 1 to 2 weeks after the start of an anticancer drug that hemoglobin reaches a nadir due to drug-attributable bone marrow suppression. Moreover, hemolysis

[11] Unpublished data.

[12] Unpublished data.
[13] Unpublished data.
[14] Unpublished data.

was unlikely considering that the study drug has a low distribution of ~8% to 11% in blood cells. The cause of the decreases in hemoglobin/anemia therefore remains unidentified. It has been reported that survivin is involved in the regulation of the proliferation of hematopoietic progenitor cells, is essential for steady-state hematopoiesis, and that the high expression of survivin is critical for proper erythroid differentiation (22). Whereas the grade 3 to 4 lymphocytopenia experienced by 7 patients in this study may be indicative of YM155-mediated effects on erythroid and lymphoid differentiation, this must be further evaluated in ongoing and future clinical studies.

Fevers occurred mainly with increase in C-reactive protein, but without significant changes in absolute neutrophil count or leukocytes. The importance of C-reactive protein is under exploration.

In the present study, the majority of study discontinuations were due to disease progression. Indeed, only one patient discontinued because of an adverse event, and this was judged not to be related to YM155. Although the evaluations of the toxicity profile of YM155 remain in the preliminary stages, the data in this study indicate that the adverse reactions observed can be well-controlled by taking due caution and suggest that YM155 has more easily controllable toxicities compared with conventional cytotoxic anticancer drugs.

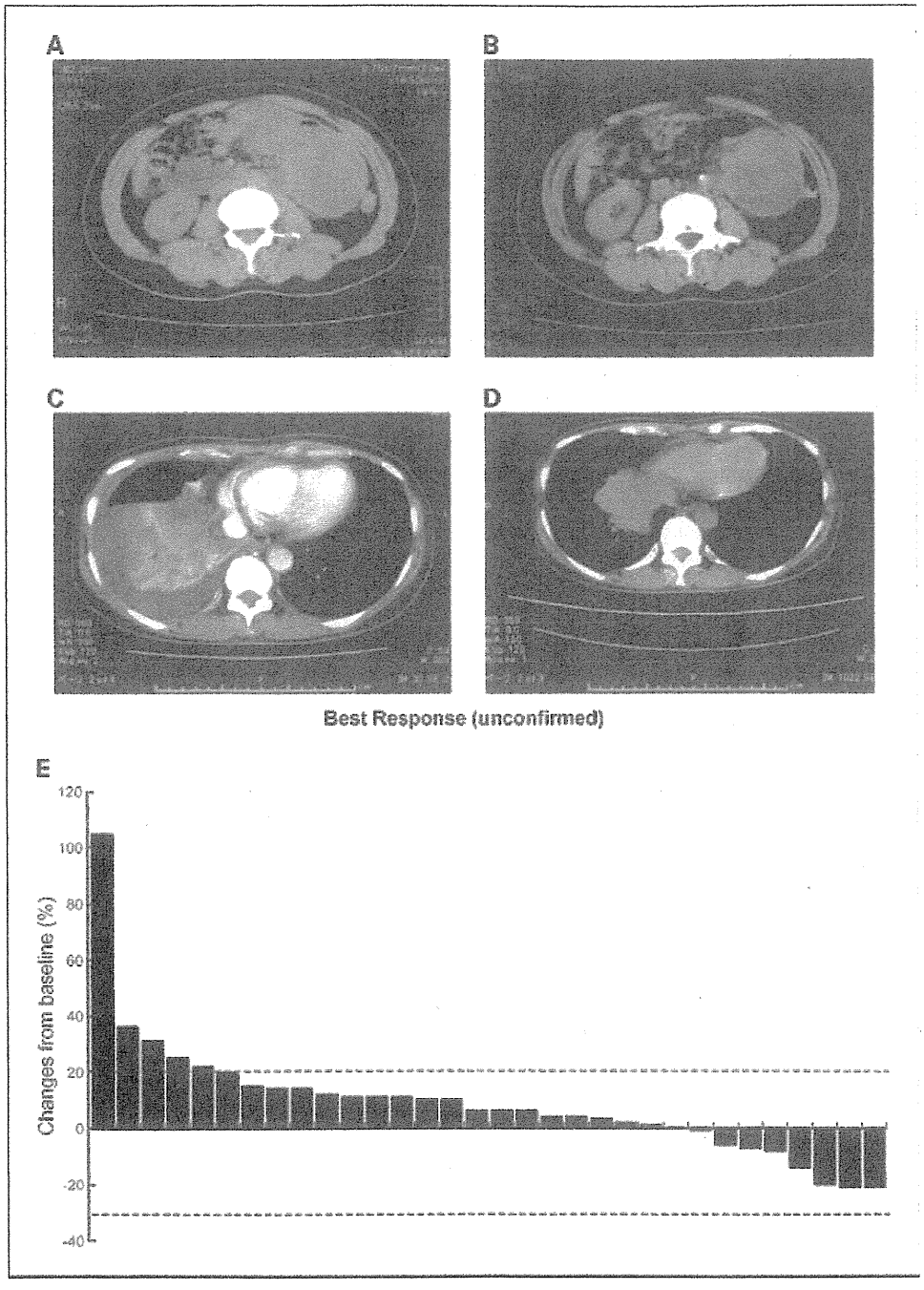

Fig. 3. Computed tomography images of a patient with malignant fibrous histiocytoma before treatment (*A*) and after (*B*).

Both $t_{1/2}$ and clearance seemed to be constant across the dose range. In addition, C_{ss} increased almost dose-proportionally (Fig. 2B), indicating the linear pharmacokinetics of YM155 over the dose range of 1.8 to 10.6 mg/m^2/d. Low concentrations of the study drug remained in systemic circulation for 48 hours after the end of infusion; however, plasma concentrations decreased to below 0.5 ng/mL before the start of cycle 2. Pharmacokinetic parameters in cycle 2 (data not shown) were similar to those in cycle 1, suggesting that there is no accumulation of study drug. We need more samples to explore the details including correlation between body surface area and pharmacokinetic parameters.

The A_e% in urine was estimated as 25% to 42% at a dose range of 1.8 to 10.6 mg/m^2/d, suggesting that urinary excretion is a principal route for the elimination of YM155. This result is well-supported by *in vitro* studies indicating that minimal metabolism of YM155 occurred in human hepatocytes (23).

The MTD of YM155 in the current study was determined to be 8.0 mg/m^2/d, after the occurrence of a DLT of increased serum creatinine in 2 of 5 patients receiving 10.6 mg/m^2/d. In contrast, in an earlier U.S. phase I trial done using the same design as the present Japanese study, the MTD was determined as 4.8 mg/m^2/d, after the occurrence of renal DLTs in 2 patients who received 6.0 mg/m^2/d (18). These DLTs were all reversible. The difference in the MTD between the U.S. and Japanese studies has been investigated by the evaluation of patient demographics, in particular baseline renal function (serum creatinine level) and prior treatment affecting renal function (history of platinum treatment), as well as hydration and pharmacokinetics of the patients with DLT. Serum creatinine levels were 1.1 and 1.4 mg/dL (reference range, 0.6-1.4 mg/dL) in the U.S. patients and 0.59 mg/dL (reference range, 0.5-1.0) and 0.81 mg/dL (reference range, 0.7-1.3 mg/dL) in the Japanese patients. Although these levels were toward the higher end of the reference range in the U.S. patients compared with those in the Japanese patients, any differences observed may be a result of two different testing facilities. Both U.S. patients had a history of platinum treatment, whereas only one of the two Japanese patients did. Furthermore, a comparison of patients receiving 6.0 mg/m^2/d of YM155 revealed that mean baseline serum creatinine levels were lower in Japanese patients than in U.S. patients. Whereas it is difficult to directly compare renal function between the two patient populations, these data do suggest that renal function may have been decreased in the U.S. patients. An additional factor to consider is body surface area. The body surface area of the U.S. patients with a DLT was 2.11 and 2.05 m^2 compared with 1.44 and 1.65 m^2 for the Japanese patients. This is suggestive of a smaller total dose of YM155. There were no essential differences between U.S. and Japanese patients in terms of the time course of plasma drug concentrations and pharmacokinetic parameters, suggesting that the difference in the MTD is unlikely to be attributable to the difference in the pharmacokinetics or exposure level.

In the present study, external evaluation showed that stable disease was achieved in nine patients. It should be noted that this prolongation of stable disease was achieved in heavily pretreated patients and response was seen also at the lowest dose. Indeed, one third of the patients had previously received four or more chemotherapy regimens. Such provocative antitumor activity in refractory solid tumors confirms the previously reported activity in the U.S. phase I trial. In the U.S. study, a partial response was achieved in 3 of 5 patients with non-Hodgkin's lymphoma and a PSA response, and a 50% reduction in 2 patients with hormone-refractory prostate cancer. Furthermore, a minor reduction (23% reduction) in tumor size was noted in one patient with non–small cell lung cancer (18). The results from both studies suggest that YM155 has promising antitumor activity against various tumor types.

In conclusion, YM155 was administered safely in this study to patients with advanced refractory solid tumors by 168-hour continuous infusion in 21-day cycles. The MTD in this patient population was determined to be 8.0 mg/m^2/d. This potential for clinical efficacy is supported by the stable responses in advanced refractory tumors achieved in this study with YM155 treatment, in addition to the antitumor activity shown in the U.S. phase I study. On the basis of the potential shown by these promising results, further randomized clinical studies of YM155 are warranted, both in the monotherapy setting and in combination regimens with established therapies.

Disclosure of Potential Conflicts of Interest

Toru Kakihara, Yumiko Aoyama, and Yohko Hashimoto are employees of Astellas Pharma, Inc.

Acknowledgments

We thank Tom van der Berg, Vincent Hofstede, Hans Mulder, and Nel Volkers (Astellas Europe B.V., Leiderdorp, the Netherlands) for bioanalysis of YM155. The authors take full responsibility for the content of the article but thank Caudex Medical (supported by Astellas Pharma) for their assistance in collating the comments of authors and other named contributors.

References

1. Ambrosini G, Adida C, Altieri DC. A novel anti-apoptosis gene, survivin, expressed in cancer and lymphoma. Nat Med 1997;3:917–21.
2. Rothe M, Pan MG, Henzel WJ, Ayres TM, Goeddel DV. The TNFR2-TRAF signaling complex contains two novel proteins related to baculoviral inhibitor of apoptosis proteins. Cell 1995;83:1243–52.
3. Roy N, Deveraux QL, Takahashi R, Salvesen GS, Reed JC. The c-IAP-1 and c-IAP-2 proteins are direct inhibitors of specific caspases. EMBO J 1997;16:6914–25.
4. Tamm I, Wang Y, Sausville E, et al. IAP-family protein survivin inhibits caspase activity and apoptosis induced by Fas (CD95), Bax, caspases, and anticancer drugs. Cancer Res 1998;58:5315–20.
5. O'Connor DS, Grossman D, Plescia J, et al. Regulation of apoptosis at cell division by p34cdc2 phosphorylation of survivin. Proc Natl Acad Sci U S A 2000;97:13103–7.
6. LaCasse EC, Baird S, Korneluk RG, MacKenzie AE. The inhibitor of apoptosis (IAPs) and their emerging role in cancer. Oncogene 1998;17:3247–59.
7. Jäättelä M. Escaping cell death: survival protein in cancer. Exp Cell Res 1999;248:30–43.
8. Lu CD, Altieri DC, Tanigawa N. Expression of a novel anti-apoptosis gene, survivin, correlated with tumor cell apoptosis and p53 accumulation in gastric carcinomas. Cancer Res 1998;58:1808–12.
9. Adida C, Berrebi D, Peuchmaur M, Reyes-Mugica M, Altieri DC. Anti-apoptosis gene, survivin, and prognosis of neuroblastoma. Lancet 1998;351:882–3.
10. Islam A, Kageyama H, Takada N, et al. High expression of Survivin, mapped to 17q25, is significantly associated with poor prognostic factors and promotes cell survival in human neuroblastoma. Oncogene 2000;19:617–23.
11. Sarela AI, Macadam RC, Farmery SM, Markham AF, Guillou PJ. Expression of the antiapoptosis gene, survivin, predicts death from recurrent colorectal carcinoma. Gut 2000;46:645–50.
12. Monzo M, Rosell R, Felip E, et al. A novel anti-apoptosis gene: reexpression of survivin messenger RNA as a prognosis marker in non-small-cell lung cancers. J Clin Oncol 1999;17:2100–4.
13. Tanaka K, Iwamoto S, Gon G, Nohara T, Iwamoto

M, Tanigawa N. Expression of survivin and its relationship to loss of apoptosis in breast carcinomas. Clin Cancer Res 2000;6:127–34.
14. Yamamoto T, Tanigawa N. The role of survivin as a new target of diagnosis and treatment in human cancer. Med Electron Microsc 2001;34: 207–12.
15. Giodini A, Kallio MJ, Wall NR, et al. Regulation of microtubule stability and mitotic progression by survivin. Cancer Res 2002;62:2462–7.
16. Mesri M, Morales-Ruiz M, Ackermann EJ, et al. Suppression of vascular endothelial growth factor-mediated endothelial cell protection by survivin targeting. Am J Pathol 2001; 158:1757–65.
17. Nakahara T, Masahiro T. YM155, a novel small-molecule survivin suppressant, induces regression of established human hormone-refractory prostate tumor xenografts. Cancer Res 2007;67:8014–21.
18. Tolcher AW, Mita A, Lewis L, et al. Phase I and pharmacokinetic study of YM155, a small molecule inhibitor of survivin. J Clin Oncol 2008;26: 5198–203.
19. Therasse P, Arbuck SG, Eisenhauer EA, et al. New guidelines to evaluate the response to treatment in solid tumors. J Natl Cancer Inst 2000;92:205–16.
20. Pennati M, Folini M, Zaffaroni N. Targeting survivin in cancer therapy. Expert Opin Ther Targets 2008;14:463–76.
21. Altieri DC. Survivin, cancer networks and pathway-directed drug discovery. Nat Rev Cancer 2008;8:61–70.
22. Leung CG, Xu Y, Mularski B, Liu H, Gurbuxani S, Crispino JD. Requirements for survivin in terminal differentiation of erythroid cells and maintenance of hematopoietic stem and progenitor cells. J Exp Med 2007;204:1603–11.
23. Sohda K, Suzuki K, Nakamura E, et al. Metabolism of YM155 monobromide, a novel survivin suppressant: *in vitro* species comparison and identification of metabolites in rats. The Proceeding of 8th International ISSX meeting 2007 (Sendai Japan). Drug Metab Rev 39:235.

Sorafenib Inhibits Non–Small Cell Lung Cancer Cell Growth by Targeting B-RAF in *KRAS* Wild-Type Cells and C-RAF in *KRAS* Mutant Cells

Ken Takezawa,[1] Isamu Okamoto,[1] Kimio Yonesaka,[1] Erina Hatashita,[1] Yuki Yamada,[1] Masahiro Fukuoka,[2] and Kazuhiko Nakagawa[1]

[1]Department of Medical Oncology, Kinki University School of Medicine; [2]Department of Medical Oncology, Kinki University School of Medicine, Sakai Hospital, Osaka, Japan

Abstract

Sorafenib is a multikinase inhibitor whose targets include B-RAF and C-RAF, both of which function in the extracellular signal-regulated kinase (ERK) signaling pathway but which also have distinct downstream targets. The relative effects of sorafenib on B-RAF and C-RAF signaling in tumor cells remain unclear, however. We have now examined the effects of sorafenib as well as of B-RAF or C-RAF depletion by RNA interference on cell growth and ERK signaling in non–small cell lung cancer (NSCLC) cell lines with or without *KRAS* mutations. Sorafenib inhibited ERK phosphorylation in cells with wild-type *KRAS* but not in those with mutant *KRAS*. Despite this difference, sorafenib inhibited cell growth and induced G_1 arrest in both cell types. Depletion of B-RAF, but not that of C-RAF, inhibited ERK phosphorylation as well as suppressed cell growth and induced G_1 arrest in cells with wild-type *KRAS*. In contrast, depletion of C-RAF inhibited cell growth and induced G_1 arrest, without affecting ERK phosphorylation, in cells with mutant *KRAS*; depletion of B-RAF did not induce G_1 arrest in these cells. These data suggest that B-RAF-ERK signaling and C-RAF signaling play the dominant roles in regulation of cell growth in NSCLC cells with wild-type or mutant *KRAS*, respectively. The G_1 arrest induced by either C-RAF depletion or sorafenib in cells with mutant *KRAS* was associated with down-regulation of cyclin E. Our results thus suggest that sorafenib inhibits NSCLC cell growth by targeting B-RAF in cells with wild-type *KRAS* and C-RAF in those with mutant *KRAS*. [Cancer Res 2009;69(16):6515–21]

Introduction

Lung cancer is the leading cause of cancer-related mortality worldwide (1). Treatment options are limited for patients with advanced metastatic lung cancer, with traditional cytotoxic chemotherapy conferring only a limited survival benefit. Target-based therapies are therefore being pursued as potential treatment alternatives. The RAS-RAF-mitogen-activated protein kinase (MAPK)/extracellular signal-regulated kinase (ERK) kinase-ERK signaling pathway is a promising therapeutic target given its central role in regulation of mammalian cell proliferation, relaying extracellular signals from ligand-bound receptor tyrosine kinases (RTK) at the cell surface to the nucleus via a cascade of specific phosphorylation events and beginning with the activation of the small GTPase RAS (2). Much attention is thus being focused on the development of inhibitors of this pathway.

RAF was the first effector kinase downstream of RAS to be identified (3). To date, the most successful clinical inhibitor of RAF activity is sorafenib (Nexavar, BAY 43-9006), an orally available compound that has received approval by the U.S. Food and Drug Administration for the treatment of advanced renal cell carcinoma and hepatocellular carcinoma. Sorafenib is also currently undergoing clinical evaluation for a variety of additional cancers, including non–small cell lung cancer (NSCLC; refs. 4–7).

The mutational status of *RAS* and *B-RAF* genes is thought to affect the sensitivity of tumor cell lines to sorafenib as a result of the inappropriate activation by such mutations of the MAPK pathway mediated by ERK (8, 9). The sensitivity of tumor cell lines with different *RAS* mutations to sorafenib is less well characterized than is that of those with *B-RAF* mutations (10–14). Despite promising results of clinical trials of sorafenib monotherapy in NSCLC patients (4–7), little is known of the possible differences in the sorafenib sensitivity of NSCLC cells according to the mutational status of *KRAS*. We have therefore now examined the effects of RAF inhibition on the growth of NSCLC cells with or without *KRAS* mutations and further investigated the mechanisms of such effects.

Materials and Methods

Cell culture and reagents. The human NSCLC cell lines NCI-H292 (H292), LK-2, Sq-1, NCI-H520 (H520), PC9, NCI-H1650 (H1650), HCC827, NCI-H1975 (H1975), A549, NCI-H460 (H460), NCI-H23 (H23), NCI-H358 (H358), and NCI-H1299 (H1299) were obtained from the American Type Culture Collection. Ma70 cells were obtained as previously described (15). All cells were cultured under a humidified atmosphere of 5% CO_2 at 37°C in RPMI 1640 (Sigma) supplemented with 10% fetal bovine serum. Sorafenib was kindly provided by Bayer Pharmaceutical, dissolved in DMSO, and stored in aliquots at −20°C.

Assay of anchorage-dependent cell growth [3-(4,5-dimethylthiazol-2-yl)-2,5-diphenyltetrazolium bromide assay]. Cells were plated in 96-well flat-bottomed plates and cultured for 24 h before exposure to various concentrations of sorafenib for 72 h. TetraColor One (5 mmol/L tetrazolium monosodium salt and 0.2 mmol/L 1-methoxy-5-methyl phenazinium methylsulfate; Seikagaku) was then added to each well, and the cells were incubated for 3 h at 37°C before measurement of absorbance at 490 nm with a Multiskan Spectrum instrument (Thermo Labsystems). Absorbance values were expressed as a percentage of that for untreated cells, and the concentration of sorafenib resulting in 50% growth inhibition (IC_{50}) was calculated.

Assay of anchorage-independent colony formation in soft agar. Anchorage-independent cell proliferation in soft agar was assayed with the use of a CytoSelect 96-Well Cell Transformation Assay (Cell Biolabs). In brief, cells were cultured for 7 d in complete medium containing soft agar and various concentrations of sorafenib. The agar matrix was then solubilized, the cells were stained with 3-(4,5-dimethylthiazol-2-yl)-2,5-diphenyltetrazolium

Requests for reprints: Isamu Okamoto, Department of Medical Oncology, Kinki University School of Medicine, 377-2 Ohno-higashi, Osaka-Sayama, Osaka 589-8511, Japan. Phone: 81-72-366-0221; Fax: 81-72-360-5000; E-mail: chi-okamoto@dotd.med.kindai.ac.jp.

doi:10.1158/0008-5472.CAN-09-1076

bromide (MTT) and lysed, and the absorbance at 570 nm was measured relative to that at a reference wavelength of 690 nm. Normalized absorbance values were expressed as a percentage of that for untreated cells, and the IC_{50} of sorafenib for inhibition of colony formation was calculated.

Cell cycle analysis. Cells were harvested, washed with PBS, fixed with 70% methanol, washed again with PBS, and stained with propidium iodide (0.05 mg/mL) in a solution containing 0.1% Triton X-100, 0.1 mmol/L EDTA, and RNase A (0.05 mg/mL). The stained cells ($\sim 1 \times 10^6$) were then analyzed for DNA content with a flow cytometer (FACSCalibur, Becton Dickinson) and ModFit software (Verity Software House).

Immunoblot analysis. Cells were washed twice with ice-cold PBS and then lysed in a solution containing 20 mmol/L Tris-HCl (pH 7.5), 150 mmol/L NaCl, 1 mmol/L EDTA, 1% Triton X-100, 2.5 mmol/L sodium pyrophosphate, 1 mmol/L phenylmethylsulfonyl fluoride, and 1 μg/mL leupeptin. The protein concentration of lysates was determined with the Bradford reagent (Bio-Rad), and equal amounts of protein were subjected to SDS-PAGE on a 7.5% gel. The separated proteins were transferred to a nitrocellulose membrane, which was then exposed to 5% nonfat dried milk in PBS for 1 h at room temperature before incubation overnight at 4°C with rabbit polyclonal antibodies to human phosphorylated ERK (1:1,000 dilution; Santa Cruz Biotechnology), ERK (1:1,000 dilution; Santa Cruz Biotechnology), FLAG epitope (1:1,000 dilution; Cell Signaling Technology), B-RAF (1:1,000 dilution; Santa Cruz Biotechnology), C-RAF (1:1,000 dilution; Cell Signaling Technology), or β-actin (1:500 dilution; Sigma) or with mouse monoclonal antibodies to cyclin E (1:1,000 dilution; Santa Cruz Biotechnology). The membrane was then washed with PBS containing 0.05% Tween 20 before incubation for 1 h at room temperature with horseradish peroxidase–conjugated goat antibodies to rabbit (Sigma) or mouse (Santa Cruz Biotechnology) immunoglobulin G. Immune complexes were finally detected with chemiluminescence reagents (Perkin-Elmer Life Science).

Forced expression of KRAS-V12. An expression vector for FLAG-tagged human KRAS-V12 was constructed by inserting the corresponding cDNA into the pcDNA3 plasmid (Invitrogen). The expression vector was introduced into H1299 cells by transfection for 48 h with the use of the Lipofectamine 2000 reagent (Invitrogen).

Gene silencing. Cells were plated at 50% to 60% confluence in six-well plates or 25-cm^2 flasks and then incubated for 24 h before transient transfection for 48 h with small interfering RNAs (siRNAs) mixed with the Lipofectamine reagent. The siRNAs specific for B-RAF (5′-AGACAGGAAUCGAAUGAAA-3′) or C-RAF (5′-CCUCACGCCUUCACCUUUA-3′) mRNAs were obtained from Dharmacon, and a nonspecific siRNA (control) was obtained from Nippon EGT. The cells were then subjected to immunoblot analysis or flow cytometry.

Statistical analysis. Data were analyzed by Student's two-tailed *t* test. A *P* value of <0.05 was considered statistically significant.

Results

Sorafenib inhibits cell growth by inducing G_1 arrest in NSCLC cell lines independently of *KRAS* genotype. The various isoforms of RAF are the principal effectors of RAS in the ERK signaling pathway, and mutant RAS proteins trigger persistent activation of downstream effectors (3). To determine whether the mutational status of *KRAS* might affect the sensitivity of NSCLC cells to sorafenib, an inhibitor of the kinase activity of RAF (16), we first examined the effects of this drug on the anchorage-dependent growth of NSCLC cells with or without *KRAS* mutations by the MTT assay. Sorafenib inhibited cell growth with IC_{50} values ranging from 7.4 to 11.3 μmol/L in NSCLC cells with wild-type *KRAS* and from 5.6 to 14.1 μmol/L in those with mutant *KRAS* (Fig. 1*A*), values that are within the clinically relevant concentration range for this drug (17). This inhibitory effect of sorafenib in cells with wild-type *KRAS* also seemed to be independent of whether the cells contained a mutant version of the *epidermal growth factor receptor* (*EGFR*) gene. We next investigated the effects of sorafenib on anchorage-independent colony formation in soft agar, a more clinically relevant model of NSCLC cell proliferation. Sorafenib inhibited anchorage-independent colony formation with IC_{50} values of 5.6 to 11.1 μmol/L in cells with wild-type *KRAS* and of 8.5 to 11.1 μmol/L in those with mutant *KRAS* (Fig. 1*B*). These data thus indicated that sorafenib inhibits the growth of NSCLC cells in a manner independent of *KRAS* mutational status.

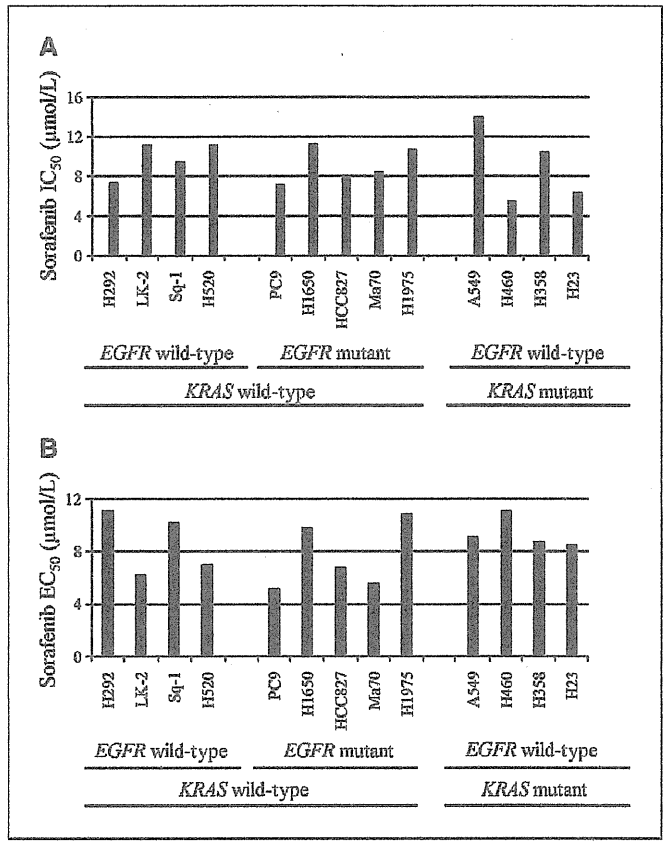

Figure 1. Effects of sorafenib on the growth of NSCLC cell lines classified according to *KRAS* and *EGFR* mutational status. *A*, the indicated NSCLC cell lines were cultured for 72 h in complete culture medium containing various concentrations of sorafenib, after which cell viability was assessed with the MTT assay and the IC_{50} values of sorafenib for inhibition of cell growth were determined. *B*, the indicated NSCLC cell lines were cultured for 7 d in complete medium containing soft agar and various concentrations of sorafenib, after which colony formation was evaluated and the IC_{50} values of sorafenib for inhibition of anchorage-independent cell proliferation were determined. All data are means of triplicates from representative experiments that were repeated on three separate occasions.

To investigate the mechanism by which sorafenib inhibits NSCLC cell growth, we examined the cell cycle profile by flow cytometry. Sorafenib increased the proportion of cells in G_1 phase of the cell cycle and reduced that of cells in S or G_2-M phases in all tested cell lines regardless of *KRAS* mutational status (Fig. 2). Sorafenib did not increase the proportion of cells in sub-G_1 phase, a characteristic of apoptosis. These data thus indicated that sorafenib inhibits cell growth by inducing arrest of the cell cycle in G_1 phase.

Effects of sorafenib on the ERK signaling pathway in NSCLC cell lines. To examine the effects of sorafenib on the ERK signaling pathway in NSCLC cells, we performed immunoblot analysis with antibodies specific for phosphorylated (activated) ERK. Sorafenib markedly inhibited ERK phosphorylation in cells with wild-type *KRAS* regardless of the mutational status of *EGFR* (Fig. 3*A*). In contrast, sorafenib had no effect on the level of ERK phosphorylation in cells

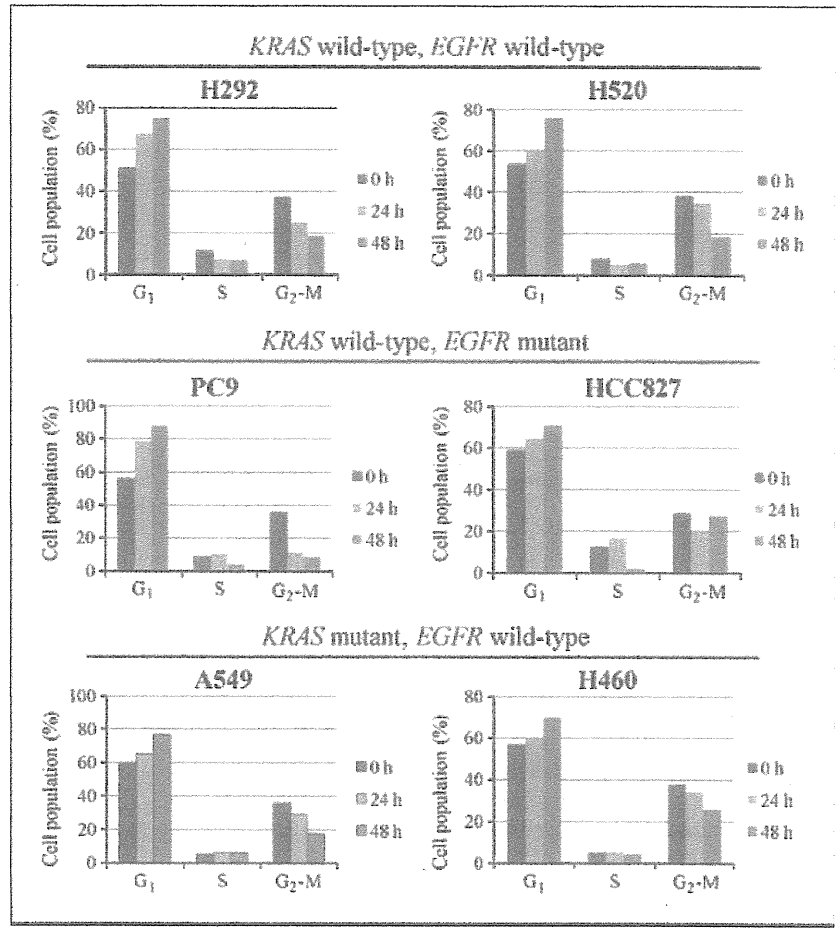

Figure 2. Effects of sorafenib on cell cycle distribution in NSCLC cells classified according to *KRAS* and *EGFR* status. Cells were incubated for 0, 24, or 48 h in complete culture medium containing 15 μmol/L sorafenib and were then fixed, stained with propidium iodide, and analyzed for cell cycle distribution by flow cytometry. All data are means of triplicates from representative experiments that were repeated on three separate occasions.

with mutant *KRAS*. To investigate further whether the effect of sorafenib on ERK phosphorylation is dependent on *KRAS* mutational status, we introduced an expression vector for FLAG epitope-tagged KRAS with the activating Val^{12} mutation (KRAS-V12) into the human NSCLC cell line H1299, which harbors wild-type endogenous *KRAS*. Whereas sorafenib inhibited ERK phosphorylation in nontransfected cells or cells transfected with the empty vector, it failed to do so in cells expressing KRAS-V12 (Fig. 3*B*). These results thus suggested that sorafenib blocks the ERK signaling pathway only in NSCLC cells harboring wild-type *KRAS*.

B-RAF but not C-RAF depletion inhibits ERK phosphorylation in NSCLC cells with wild-type or mutant KRAS. The mammalian RAF family includes A-RAF, B-RAF, and C-RAF, all of which function in the ERK pathway but also have different downstream phosphorylation targets and play distinct roles in signaling (18). Although suggested to be a B-RAF inhibitor, sorafenib inhibits the activity of C-RAF with a potency 4-fold that apparent for B-RAF (16). To investigate the downstream consequences of B-RAF and C-RAF signaling in NSCLC cells, we examined the effects of the depletion of these kinases with a siRNA-based approach. Immunoblot analysis revealed

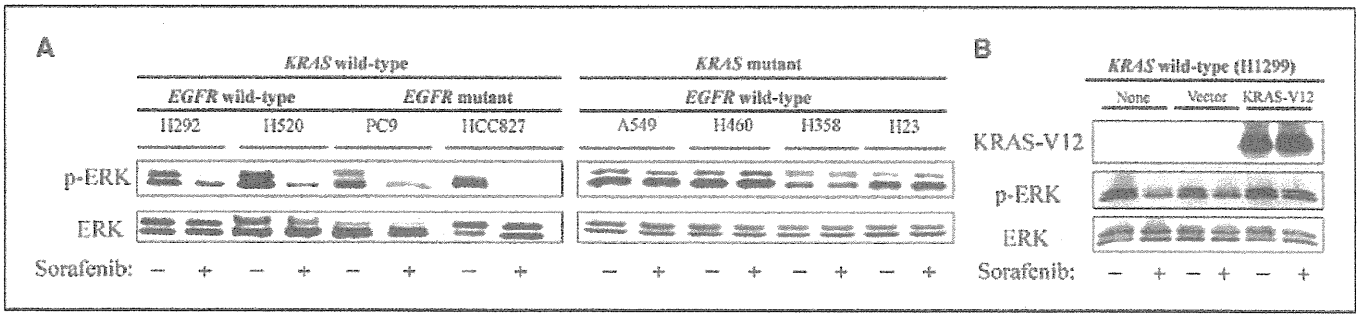

Figure 3. Effects of sorafenib on ERK phosphorylation in NSCLC cells classified according to *KRAS* and *EGFR* status. *A*, cells were incubated for 2 h in the presence or absence of sorafenib (15 μmol/L), after which cell lysates (25 μg of soluble protein) were subjected to immunoblot analysis with antibodies to phosphorylated (*p-ERK*) or total forms of ERK. *B*, H1299 cells were transiently transfected (or not) for 48 h with an expression vector for FLAG-tagged KRAS-V12 or with the corresponding empty vector and were then incubated for 2 h in the presence or absence of sorafenib (15 μmol/L). Cell lysates (25 μg of soluble protein) were then subjected to immunoblot analysis with antibodies to FLAG and to phosphorylated or total forms of ERK.

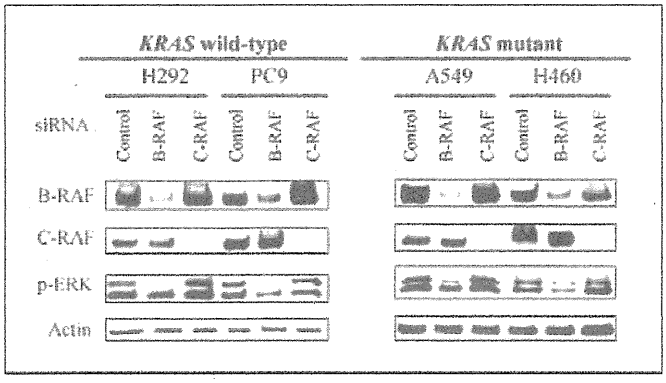

Figure 4. Effects of transient depletion of B-RAF or C-RAF on ERK phosphorylation in NSCLC cells. Cells harboring wild-type or mutant *KRAS* were transfected with nonspecific (control), B-RAF, or C-RAF siRNAs for 48 h, after which cell lysates were prepared and subjected to immunoblot analysis with antibodies to B-RAF, C-RAF, phosphorylated ERK, and β-actin (loading control).

that transfection of NSCLC cells with siRNAs specific for B-RAF or C-RAF mRNAs resulted in marked and selective depletion of the corresponding protein (Fig. 4). Such depletion of B-RAF resulted in inhibition of ERK phosphorylation in cells harboring wild-type or mutant *KRAS*, whereas depletion of C-RAF had no such effect (Fig. 4). These data thus suggested that depletion of B-RAF, but not that of C-RAF, inhibits ERK phosphorylation regardless of *KRAS* status.

Effects of RAF depletion on NSCLC cell proliferation. We next examined the effects of B-RAF or C-RAF depletion on NSCLC cell proliferation and cell cycle distribution. Depletion of B-RAF resulted in significant inhibition of cell proliferation (Fig. 5*A*) and an increase in the proportion of cells in G_1 phase of the cell cycle (Fig. 5*B*), whereas depletion of C-RAF had no such effects, in NSCLC cells harboring wild-type *KRAS*. In contrast, depletion of C-RAF induced significant inhibition of cell proliferation (Fig. 5*A*) and an increase in the proportion of cells in G_1 phase (Fig. 5*B*), whereas depletion of B-RAF had only a less pronounced effect on cell proliferation, in NSCLC cells with mutant *KRAS*. These data thus suggested that B-RAF-ERK signaling regulates cell proliferation in NSCLC cells with wild-type *KRAS*, whereas C-RAF signaling mediates such regulation in NSCLC cells with mutant *KRAS*.

Sorafenib or C-RAF depletion inhibits cyclin E expression in NSCLC cells with mutant *KRAS*. Finally, to characterize further the growth inhibition and G_1 arrest induced by C-RAF depletion or sorafenib in NSCLC cells with mutant *KRAS*, we examined the expression of cyclin E, an essential promoter of the transition from G_1 to S phase of the cell cycle (19). Immunoblot analysis revealed that depletion of C-RAF in A549 or H460 cells resulted in pronounced inhibition of cyclin E expression, whereas depletion of B-RAF had no such effect (Fig. 6). Exposure of the cells to sorafenib also induced loss of cyclin E (Fig. 6). These results thus suggest that the G_1 arrest induced by depletion of C-RAF or by sorafenib in NSCLC cells with mutant *KRAS* may be attributable to the down-regulation of cyclin E.

Discussion

RAS is an upstream component of the ERK signaling pathway, which is aberrantly activated by oncogenic mutations of RAS genes. Among RAS family genes, mutations of *KRAS* are most common in solid malignancies, including NSCLC (8, 20, 21). Indeed, *KRAS* mutations have been associated with poor prognosis and resistance to conventional cytotoxic chemotherapy in NSCLC (22–24). Whereas EGFR tyrosine kinase inhibitors are most efficacious in NSCLC patients with *EGFR* mutations, *KRAS* mutations are associated with resistance to these agents (25–28). The development of therapeutic strategies for NSCLC patients with *KRAS* mutations is thus an important clinical goal. RAF serine-threonine kinases are the principal effectors of RAS in the ERK signaling pathway. Given the key role of this pathway in tumor growth, RAF is a potential target for cancer therapy.

Sorafenib is an orally available compound that has been developed as a multikinase inhibitor with activity against RAF and several RTKs. The sensitivity of cancer cells to sorafenib might be expected to be affected by *KRAS* status, given that *KRAS* mutations result in activation of the ERK pathway (8). However, as far as we are aware, no previous study has compared sorafenib sensitivity among a panel of tumor cell lines of different *KRAS* mutational status. We have now evaluated the effects of sorafenib on the growth of NSCLC cells harboring wild-type or mutant forms of *KRAS* with two different assay systems, the MTT assay and anchorage-independent colony formation assay, given that previous studies have revealed differences in the sensitivity of cells to tested drugs between these two assay systems (29). The IC_{50} values for inhibition of cell growth by sorafenib in these assays have generally been found to be well below 15 μmol/L, the maximum achievable plasma concentration of this drug (17). We found that the potency of sorafenib for inhibition of cell growth was similar for NSCLC cells regardless of *KRAS* mutational status in both assay systems. We also performed a longer-term clonogenic survival assay and again found that sorafenib inhibited the survival of NSCLC cells regardless of *KRAS* status (data not shown). These results thus indicate that sorafenib inhibits the growth of NSCLC cells with mutant *KRAS* as well as it does that of those with wild-type *KRAS* in a clinically relevant concentration range.

We have shown that sorafenib inhibited ERK phosphorylation and induced G_1 arrest in NSCLC cells with wild-type *KRAS*, consistent with previous results obtained with several cancer cell lines harboring wild-type *KRAS* (13, 30, 31). Inhibition of the ERK signaling pathway, as reflected by a reduced level of ERK phosphorylation, results in inhibition of cell proliferation and induction of G_1 arrest in various cell types (32–35). In the present study, we found that depletion of B-RAF by RNA interference also inhibited ERK phosphorylation as well as attenuated cell proliferation and induced G_1 arrest in NSCLC cells with wild-type *KRAS*. These results suggest that inhibition of B-RAF-ERK signaling contributes to suppression of the growth of NSCLC cells harboring wild-type *KRAS* by sorafenib. Consistent with these findings, the specific B-RAF inhibitor SB-590885 was previously shown to inhibit ERK phosphorylation and to induce G_1 arrest in melanoma cells with wild-type *KRAS* (36, 37). In contrast, we found that depletion of C-RAF did not result in inhibition of ERK phosphorylation in NSCLC cells. ERK activation was previously shown to be conserved in cells derived from C-RAF knockout mice, suggesting that C-RAF is dispensable for ERK signaling (38, 39). Together, the present data suggest that B-RAF-ERK signaling, rather than C-RAF signaling, is a potential therapeutic target in NSCLC cells with wild-type *KRAS*.

We showed that ERK phosphorylation was not inhibited by sorafenib in two NSCLC cell lines (A549 and H460) harboring mutant *KRAS*, consistent with previous observations (16). We further showed this to be the case in two additional such cell lines (H358 and H23). Such results were previously suggested to be due to the existence of RAF-independent ERK activation in

NSCLC cells with mutant *KRAS* (16). However, we have now shown that B-RAF depletion resulted in inhibition of ERK activation in these cells. Our data therefore suggest that sorafenib is not able to attenuate the constitutive activation of the B-RAF-ERK pathway characteristic of NSCLC cells harboring mutant *KRAS* (40). Despite the sustained activation of B-RAF-ERK signaling in such cells, sorafenib inhibited cell proliferation and induced G_1 arrest in NSCLC cells with mutant *KRAS* as well as in those with wild-type *KRAS*. These data suggest that sorafenib targets a different pathway in its inhibitory effect on cell growth in NSCLC cells with mutant *KRAS*. Whereas sorafenib inhibits the kinase activity of both B-RAF and C-RAF, it shows a higher affinity for C-RAF (16). We found that depletion of C-RAF by RNA interference inhibited cell proliferation and induced G_1 arrest, without affecting ERK phosphorylation, in NSCLC cells with mutant *KRAS*, whereas it did not exhibit such effects in NSCLC cells harboring wild-type *KRAS*. Depletion of B-RAF also inhibited the growth of NSCLC cells with mutant *KRAS*, although this effect was not as pronounced as that in those with wild-type *KRAS*. These data indicate that NSCLC cells with mutant *KRAS* are dependent on C-RAF signaling to a greater extent than on B-RAF-ERK signaling for cell proliferation but that both pathways participate in regulation of the growth of these cells. Melanoma cells that have acquired resistance to a specific B-RAF inhibitor were recently shown to have switched their dependency from B-RAF to C-RAF (41). These observations suggest that RAF proteins are functionally interchangeable in the regulation of cell growth. Our data thus indicate that C-RAF signaling is a potential therapeutic target in NSCLC cells with mutant *KRAS*. RAF family proteins are also implicated in regulation of cell cycle progression in a manner independent of the ERK pathway (18, 38, 42, 43). C-RAF has been shown to exist in a complex with Cdc25, which activates the cyclin E-Cdk2 complex and promotes the G_1-S phase transition (44, 45). Cyclin E is thus postulated to be a downstream effector of C-RAF. In the present study, we found that either C-RAF depletion or sorafenib treatment induced G_1 arrest and down-regulation of cyclin E in NSCLC cells with mutant *KRAS*. Although we cannot exclude a possible role for other cell cycle

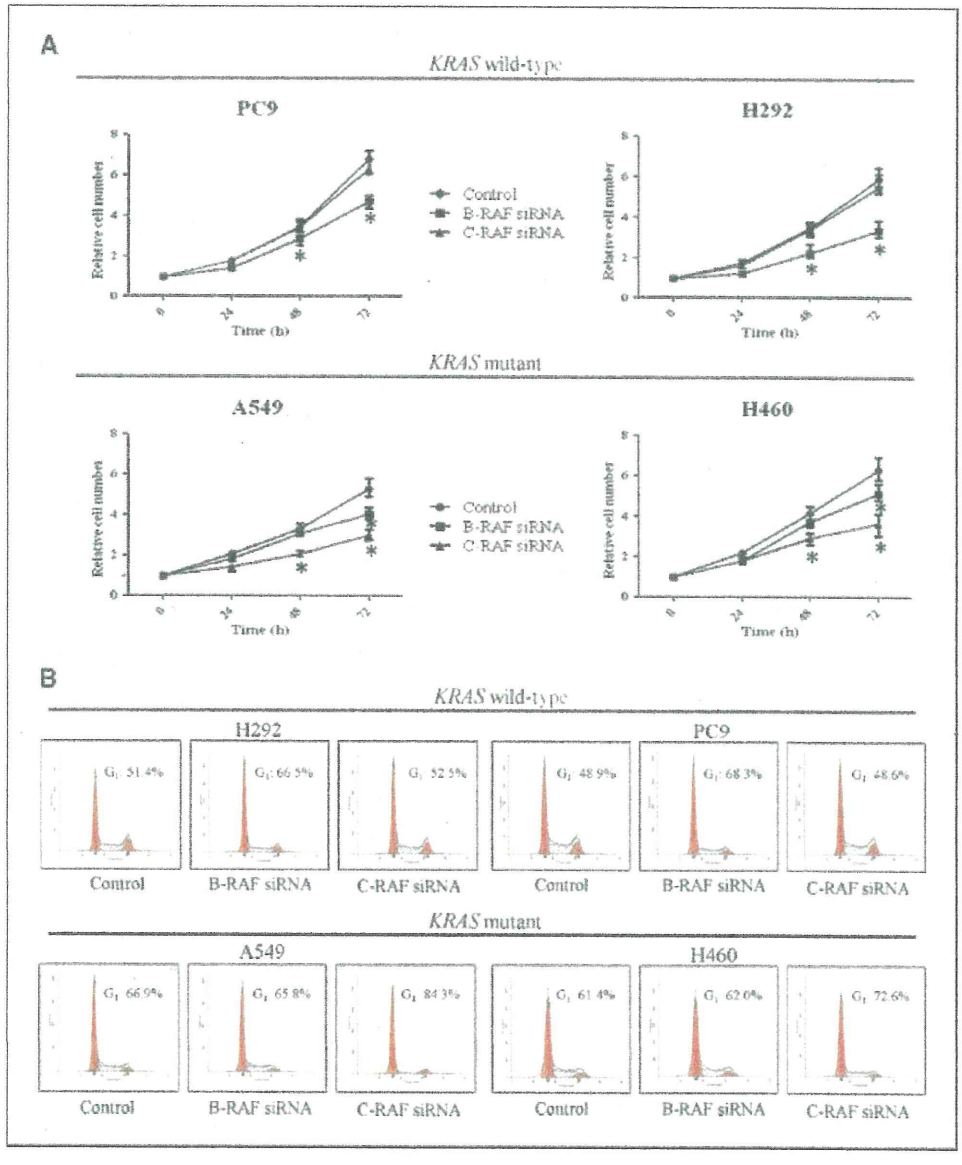

Figure 5. Effects of B-RAF or C-RAF depletion on cell proliferation and cell cycle distribution in NSCLC cells. *A*, cells harboring wild-type or mutant *KRAS* were transfected with nonspecific (control), B-RAF, or C-RAF siRNAs for the indicated times, after which the number of viable cells was determined by staining with trypan blue. The number of viable cells is expressed relative to the value for time 0. *Points*, mean values from three independent experiments; *bars*, SD. *, $P < 0.05$ versus the corresponding value for cells transfected with the nonspecific siRNA. *B*, cells were transfected as in *A* for 48 h, fixed, stained with propidium iodide, and analyzed for cell cycle distribution by flow cytometry. The percentage of cells in G_1 phase is indicated. Data are from representative experiments that were repeated on three separate occasions.

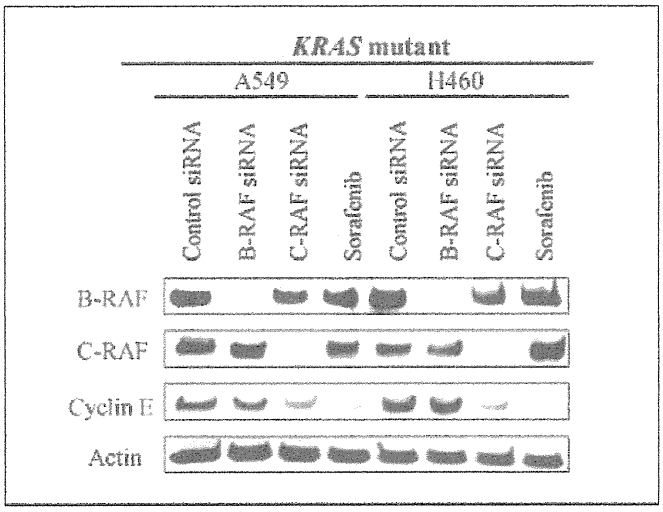

Figure 6. Effects of C-RAF depletion or sorafenib on cyclin E expression in NSCLC cells with mutant *KRAS*. Cells harboring mutant *KRAS* were transiently transfected for 48 h with nonspecific (control), B-RAF, or C-RAF siRNAs or were exposed to 15 μmol/L sorafenib for 24 h in complete medium. Cell lysates were then prepared and subjected to immunoblot analysis with antibodies to B-RAF, C-RAF, cyclin E, and β-actin.

proteins, our present data suggest that the observed down-regulation of cyclin E may contribute to the G_1 arrest induced by C-RAF depletion or by sorafenib in NSCLC cells with mutant *KRAS*.

Sorafenib inhibits several RTKs that participate in neovascularization, including vascular endothelial growth factor receptor (VEGFR)-2 and VEGFR-3 (16). Inhibition of angiogenesis might thus be expected to contribute to the inhibition of tumor growth by this drug in addition to its effects on RAF signaling. Although sorafenib was previously shown to inhibit the growth of a variety of human tumor xenografts in mice (13, 16, 46), it has been difficult to measure the relative contributions of its antiangiogenic activity and its direct antitumor activity mediated by RAF inhibition. In the present study, we have provided insight into the inhibitory effect of sorafenib on tumor cell growth *in vitro* that is mediated by inhibition of RAF signaling pathways. Our results suggest that sorafenib targets B-RAF in NSCLC cells with wild-type *KRAS* and C-RAF in those with mutant *KRAS*, and they provide a rationale for future clinical investigation of the therapeutic efficacy of sorafenib for NSCLC patients.

Disclosure of Potential Conflicts of Interest

No potential conflicts of interest were disclosed.

Acknowledgments

Received 3/23/09; revised 5/22/09; accepted 6/15/09; published OnlineFirst 7/28/09.

The costs of publication of this article were defrayed in part by the payment of page charges. This article must therefore be hereby marked *advertisement* in accordance with 18 U.S.C. Section 1734 solely to indicate this fact.

We thank H. Saya, K. Nishio, and T. Arao for helpful discussion.

References

1. Jemal A, Siegel R, Ward E, et al. Cancer statistics, 2008. CA Cancer J Clin 2008;58:71–96.
2. Eccles SA. Parallels in invasion and angiogenesis provide pivotal points for therapeutic intervention. Int J Dev Biol 2004;48:583–98.
3. Sridhar SS, Hedley D, Siu LL. Raf kinase as a target for anticancer therapeutics. Mol Cancer Ther 2005;4:677–85.
4. Adjei AA, Hillman SL. A front-line window of opportunity phase II study of sorafenib in patients with advanced non-small cell lung cancer: a North Central Cancer Treatment Group Study. Proc Am Soc Clin Oncol 2007;25:S18.
5. Gatzemeier U, Fosella F. Phase II trial of singe-agent sorafenib in patients with advanced non-small cell lung carcinoma. J Clin Oncol 2006;24:7002.
6. Gutierrez SKM, Allen D, Turkbey B, et al. A phase II study of multikinase inhibitor sorafenib in patients with relapsed non-small cell lung cancer [abstract 19084]. J Clin Oncol 2008;26:S712.
7. Schiller JH, Hanna NH, Traynor AM, Carbone DP. A randomized discontinuation phase II study of sorafenib versus placebo in patients with non-small cell lung cancer who have failed at least two prior chemotherapy regimens [abstract 8014]. J Clin Oncol 2008;26:S427.
8. Rodenhuis S, van de Wetering ML, Mooi WJ, Evers SG, van Zandwijk N, Bos JL. Mutational activation of the K-ras oncogene. A possible pathogenetic factor in adenocarcinoma of the lung. N Engl J Med 1987;317:929–35.
9. Garnett MJ, Marais R. Guilty as charged: B-RAF is a human oncogene. Cancer Cell 2004;6:313–9.
10. Panka DJ, Wang W, Atkins MB, Mier JW. The Raf inhibitor BAY 43-9006 (sorafenib) induces caspase-independent apoptosis in melanoma cells. Cancer Res 2006;66:1611–9.
11. Molhoek KR, Brautigan DL, Slingluff CL, Jr. Synergistic inhibition of human melanoma proliferation by combination treatment with B-Raf inhibitor BAY43-9006 and mTOR inhibitor rapamycin. J Transl Med 2005;3:39.
12. Lasithiotakis KG, Sinnberg TW, Schittek B, et al. Combined inhibition of MAPK and mTOR signaling inhibits growth, induces cell death, and abrogates invasive growth of melanoma cells. J Invest Dermatol 2008;128:2013–23.
13. Henderson YC, Ahn SH, Kang Y, Clayman GL. Sorafenib potently inhibits papillary thyroid carcinomas harboring RET/PTC1 rearrangement. Clin Cancer Res 2008;14:4908–14.
14. Smalley KS, Xiao M, Villanueva J, et al. CRAF inhibition induces apoptosis in melanoma cells with non-V600E BRAF mutations. Oncogene 2009;28:85–94.
15. Okabe T, Okamoto I, Tamura K, et al. Differential constitutive activation of the epidermal growth factor receptor in non-small cell lung cancer cells bearing EGFR gene mutation and amplification. Cancer Res 2007;67:2046–53.
16. Wilhelm SM, Carter C, Tang L, et al. BAY 43-9006 exhibits broad spectrum oral antitumor activity and targets the RAF/MEK/ERK pathway and receptor tyrosine kinases involved in tumor progression and angiogenesis. Cancer Res 2004;64:7099–109.
17. Strumberg D, Clark JW, Awada A, et al. Safety, pharmacokinetics, and preliminary antitumor activity of sorafenib: a review of four phase I trials in patients with advanced refractory solid tumors. Oncologist 2007;12:426–37.
18. Wojnowski L, Stancato LF, Larner AC, Rapp UR, Zimmer A. Overlapping and specific functions of Braf and Craf-1 proto-oncogenes during mouse embryogenesis. Mech Dev 2000;91:97–104.
19. Dobashi Y. Cell cycle regulation and its aberrations in human lung carcinoma. Pathol Int 2005;55:95–105.
20. Buttitta F, Barassi F, Fresu G, et al. Mutational analysis of the HER2 gene in lung tumors from Caucasian patients: mutations are mainly present in adenocarcinomas with bronchioloalveolar features. Int J Cancer 2006;119:2586–91.
21. Suzuki M, Shigematsu H, Iizasa T, et al. Exclusive mutation in epidermal growth factor receptor gene, HER-2, and KRAS, and synchronous methylation of nonsmall cell lung cancer. Cancer 2006;106:2200–7.
22. Graziano SL, Gamble GP, Newman NB, et al. Prognostic significance of K-ras codon 12 mutations in patients with resected stage I and II non-small-cell lung cancer. J Clin Oncol 1999;17:668–75.
23. Slebos RJ, Kibbelaar RE, Dalesio O, et al. K-ras oncogene activation as a prognostic marker in adenocarcinoma of the lung. N Engl J Med 1990;323:561–5.
24. Winton T, Livingston R, Johnson D, et al. Vinorelbine plus cisplatin vs. observation in resected non-small-cell lung cancer. N Engl J Med 2005;352:2589–97.
25. Pao W, Wang TY, Riely GJ, et al. KRAS mutations and primary resistance of lung adenocarcinomas to gefitinib or erlotinib. PLoS Med 2005;2:e17.
26. Massarelli E, Varella-Garcia M, Tang X, et al. KRAS mutation is an important predictor of resistance to therapy with epidermal growth factor receptor tyrosine kinase inhibitors in non-small-cell lung cancer. Clin Cancer Res 2007;13:2890–6.
27. Marks JL, Broderick S, Zhou Q, et al. Prognostic and therapeutic implications of EGFR and KRAS mutations in resected lung adenocarcinoma. J Thorac Oncol 2008;3:111–6.
28. Baselga J, Rosen N. Determinants of RASistance to anti-epidermal growth factor receptor agents. J Clin Oncol 2008;26:1582–4.
29. Hao H, Muniz-Medina VM, Mehta H, et al. Context-dependent roles of mutant B-Raf signaling in melanoma and colorectal carcinoma cell growth. Mol Cancer Ther 2007;6:2220–9.
30. Jane EP, Premkumar DR, Pollack IF. Coadministration of sorafenib with rottlerin potently inhibits cell proliferation and migration in human malignant glioma cells. J Pharmacol Exp Ther 2006;319:1070–80.
31. Ambrosini G, Cheema HS, Seelman S, et al. Sorafenib inhibits growth and mitogen-activated protein kinase signaling in malignant peripheral nerve sheath cells. Mol Cancer Ther 2008;7:890–6.
32. Villanueva J, Yung Y, Walker JL, Assoian RK. ERK activity and G_1 phase progression: identifying dispensable versus essential activities and primary versus secondary targets. Mol Biol Cell 2007;18:1457–63.